Supporting Information

Maximizing Hydrogen Utilization Efficiency in Tandem Hydrogenation of Nitroarenes with Ammonia Borane

Mengqi Shen,[1,2‡] Christoph Bendel,[3‡] Hunter B. Vibbert,[1,2] Pan Thi Khine,[4] Jack R. Norton,[3*] and Aaron J. Moment[4*]

[1]Lenfest Center for Sustainable Energy, Columbia University, New York, NY 10027, USA.

[2]Department of Earth and Environmental Engineering, Columbia University, New York, NY 10027, USA.

[3]Department of Chemistry, Columbia University, New York, NY 10027, USA.

[4]Department of Chemical Engineering, Columbia University, New York, NY 10027, USA.

* Jack R. Norton - Email: jrn11@columbia.edu

* Aaron J. Moment - Email: ajm2293@columbia.edu

‡These authors contributed equally.

Contents

1. Methods 2
2. Supplementary Table 4
3. Supplementary Fig. S1-4 5
4. Supplementary Scheme S1 8
Product Characterization 9
NMR Spectra 13
References 33

1. Methods

Chemicals and Materials. All commercial reagents were used as received without further purification. Ammonia borane (AB, 97 %), nitroarenes, borane tert-butylamine complex (BBA, 97%), oleylamine (OAm, > 70%), oleic acid (OAc, 90%), copper (II) acetylacetonate ($Cu(acac)_2$, 97 %), and nickel (II) acetylacetonate ($Ni(acac)_2$, 95 %) were purchased from Sigma-Aldrich. Pd/C (10 wt %) catalyst and all the solvents were from Fisher Scientific.

Batch tandem hydrogenation reactions. In a typical nitrobenzene reduction, nitrobenzene (1 mmol), Pd/C (10 wt %) catalyst (1 mol % Pd), and methanol (5 mL) were placed in a two-neck round bottom flask (50 mL) with a stir bar. One neck was connected to a balloon, the other neck was sealed by a rubber stopper. A solution of AB (1.04 mmol) in methanol (5 mL) was rapidly injected into the flask from the rubber stopper neck. After 30 min, the catalyst was separated from the suspension by centrifugation, and the reaction solution was analyzed by GC-MS and NMR spectroscopy.

Continuous-flow tandem hydrogenation reactions. The continuous-flow reactions were conducted in an H-Cube® mini plus flow reactor (ThalesNano). Pd/C (10 wt %) catalyst (80 mg) was packed into the reaction column. In a typical reduction, nitrobenzene (10 mmol), AB (10.4 mmol), and 1,3,5-trimethoxybenzene (4 mmol) were dissolved in methanol (40 mL) and pumped onto the catalyst column with an inlet flow rate of 1 mL·min^{-1} at ambient temperature and pressure. The product solution was collected from the outlet and analyzed by GC-MS and NMR spectroscopy.

Mole ratio (χ) calculation.

Within a given volume inside the column,

$$\chi = \frac{mol_{Pd}}{c_s \cdot V_c}$$

mol_{Pd} = mol of Pd in the reaction column, c_s = substrate concentration (mol·L^{-1}), V_c = the free space in the column (L).

Within a given time,

$$\chi = \frac{mol_{Pd}}{c_s \cdot Q_s \cdot t}$$

$mole_{Pd}$ = mol of Pd in the reaction colum, c_s = substrate concentration (mol·L^{-1}), Q_s = the flow rate (L·min^{-1}), t = overall working time (min).

Space-Time Yield (STY) calculation. The STYs were calculated as previously described.[S1]

For the batch reaction,

$$STY_{batch} = c_p \cdot \frac{M_p}{t}$$

c_p= product concentration (mol·L^{-1}), M_p = molar mass of the product (g·mol^{-1}), t = process time (min).

For the flow reaction,

$$STY_{flow} = c_{p,outlet} \cdot \frac{M_p}{t}$$

$c_{p,outlet}$= product concentration from the outlet (mol·L^{-1}), M_p = molar mass of the product (g·mol^{-1}), t= process time in the column (min).

Synthesis of CuNi NPs. CuNi NPs were prepared according to the literature.[S2] 0.13 mmol of $Cu(acac)_2$ and 0.26 mmol of $Ni(acac)_2$ were added into a three-neck flask with 7.5 mL of OAm and 0.16 mL of OAc under magnetic stirring in the Ar atmosphere. The formed solution was heated to 383 K and degassed for 0.5 h to remove moisture and oxygen. The reaction solution was further heated to 473 K quickly (ramp rate of 20 K/min) and 160 mg of BBA (in 1 mL of OAm) was quickly injected into the solution. The reaction was kept at 473 K for 30 min and cooled to room temperature. 100 mL ethanol was added, and the NP product was separated by centrifugation at 8000 rpm for 10 min. The NPs were washed twice with hexane/ethanol (v/v= 1:15).

Characterization. NMR spectra were recorded using a Bruker Avance III 400 or 400SL spectrometer. Coupling constants *J* were given in Hertz (Hz) and chemical shifts δ were reported in parts per million (ppm). For labeling of signals in ^1H NMR spectra, the abbreviations s = singlet, d = doublet, t = triplet, q = quartet, m = multiplet, and br = broad signal were used. GC-MS was recorded on an Agilent 7890B GC System 5977B MSD GC-MS with an EI ionization method. Continuous flow reactions were conducted in the H-Cube® mini plus (THALESNano). Transmission electron microscopy (TEM) images were taken from an FEI TALOS F200X at 200 kV. X-ray diffraction (XRD) patterns were collected on a PANALYTICAL XPERT3 powder diffractometer with a 3 kW generator, fully ceramic Cu Long fine focus (LFF), X-ray tube, vertical goniometer (theta-theta), and a PIXcel 1d detector.

Kinetic and Reaction Modeling. The tandem chemical reactions were simulated using Aspen Plus V8.8 software package. In this simulation, trimethylamine borane was used instead of ammonia borane as it was not available in the component database of Aspen. Therefore, the two reactions for the tandem nitrobenzene reaction became:

$$(CH)_3NBH_3 + 3\ CH_3OH \rightarrow 3\ H_2 + B(OCH_3)_3 + N(CH_3)_3$$

$$C_6H_5NO_2 + 3\ H_2 \rightarrow C_6H_5NH_2 + 2\ H_2O$$

The components used were trimethylamine borane, methanol, hydrogen, trimethyl borate, trimethyl amine, nitrobenzene, aniline, and water. For the methods, "COMMONS" was used as the method filter and "NRTL" was used as the base method. The reaction was simulated in a RPlug reactor, with the dimensions of 22.0 mm in length and 3.8 mm in width. Its temperature was specified at 25 ℃, and was set up with 0.01 kg of catalyst loading with 0.5 bed voidage. The temperature of input stream was at 25 ℃ and the reaction pressure was set to 1 bar.

Two separate reactions as mentioned above were put into one reaction set. As they are both surface reactions, LHHW was selected as the reaction type, and the stoichiometry was entered the same as the chemical equations. In addition, only the second reaction was set as the reversible reaction, and the rate basis was on catalyst weight. The below equations give the rate laws for the first and second reactions, respectively.

$$r_1 = \frac{k_1[(CH)_3NBH_3][CH_3OH]^3}{(1 + K_1[(CH)_3NBH_3] + K_2[CH_3OH] + K_3[H_2] + K_4'[B(OCH_3)_3] + K_5'[N(CH_3)_3] + K_6[}$$

$$r_2 = \frac{k_2[C_6H_5NO_2][H_2]^3}{(1 + K_1[(CH)_3NBH_3] + K_2[CH_3OH] + K_3[H_2] + K_4'[B(OCH_3)_3] + K_5'[N(CH_3)_3] + K_6[}$$

Where:

K = equilibrium constant

K' = 1/K

The kinetic expression for the rate equation in Aspen is given as:

$$r = \frac{[kinetic\ factor][Driving\ force]}{[adsorption]}$$

The derived rate law is broken down into kinetic factor term, driving force term, and adsorption term. The required coefficients for driving force constants for driving force term, and adsorption constants for the adsorption term were adjusted empirically to obtain the similar conversions as given from the lab experiments. Table S3-S4 illustrates the values for kinetic factors and the driving force term.

2. Supplementary Table

Table S1. Heterogeneous catalysts for tandem hydrogenation of nitroarenes with AB

Entry	Cat.	AB (equiv.)	Yield (%)	STY ($gL^{-1}min^{-1}$)	Ref.
1	Pd/C in flow	1	99	**92.07**	**This work**
2	CuNi NPs in flow	1	90	**3.68**	**This work**
3	CuNi NPs	3	99	0.3	S3
4	NiPd NPs	**1**	**10**	0.0006	S4
5	NiPd NPs	3	99	1.84	S4
6	Pd/MOF	5	99	0.25	S5
7	Rh@S-1-H	10	99	0.34	S6
8	Rh/C	10	99	0.17	S6
9	AuPd NPs	2	99	0.31	S7
10	CuPd NPs	3	99	0.13	S8
11	PtZn/HNCNT	6	99	0.05	S9
12	PtPd NPs	9.7	99	0.005	S10
13	mpg-C_3N_4/Pd	2.86	95	6.19	S11
14	FePd NPs	3	99	0.92	S12
15	Pd@MIL-101	2.19	99	1.23	S13
16	CuO	**1**	**35**	0.27	S14
17	CuO	3	93	0.72	S14
18	CoNi/Al_2O_3	4	99	0.06	S15

Table S2. Heterogeneous catalysts for tandem hydrogenation of nitroarenes with AB

Entry	Cat.	AB (equiv.)	Yield (%)	STY ($gL^{-1}min^{-1}$)	Ref.
1	Pd/C in flow	1	99	**92.07**	**This work**
2	CuNi NPs in flow	1	90	**3.68**	**This work**
3	CuNi NPs	3	99	0.3	S3
4	NiPd NPs	**1**	**10**	0.0006	S4
5	NiPd NPs	3	99	1.84	S4
6	Pd/MOF	5	99	0.25	S5
7	Rh@S-1-H	10	99	0.34	S6
8	Rh/C	10	99	0.17	S6
9	AuPd NPs	2	99	0.31	S7
10	CuPd NPs	3	99	0.13	S8
11	PtZn/HNCNT	6	99	0.05	S9
12	PtPd NPs	9.7	99	0.005	S10
13	mpg-C_3N_4/Pd	2.86	95	6.19	S11
14	FePd NPs	3	99	0.92	S12
15	Pd@MIL-101	2.19	99	1.23	S13
16	CuO	**1**	**35**	0.27	S14
17	CuO	3	93	0.72	S14
18	CoNi/Al_2O_3	4	99	0.06	S15

Table S3. Driving Force and Kinetic Factor Parameters for Reaction Model

			Reaction 1		Reaction 2	
				unit		unit
kinetic factor		k	0.115		35	
		n	1		0	
		E	5	kJ/mol	8.2	kJ/mol
		To	25	℃	25	℃
Driving force	concentration exponents in forward reaction rate	trimethylamine borane	1		N/A	
		methanol	3		N/A	
		hydrogen	0		3	
		trimethyl borate	0		N/A	
		trimethyl amine	0		N/A	
		nitrobenzene	N/A		1	
		aniline	N/A		0	
		water	N/A		0	
	coefficients for driving force constant in forward reaction rate	A	N/A		10.25	
		B	N/A		998	
		C	N/A		0	
		D	N/A		0	
	concentration exponents in reverse reaction rate	trimethylamine borane	N/A		N/A	
		methanol	N/A		N/A	
		hydrogen	N/A		0	
		trimethyl borate	N/A		N/A	
		trimethyl amine	N/A		N/A	
		nitrobenzene	N/A		0	
		aniline	N/A		0	
		water	N/A		0	
	coefficients for driving force constant in reverse reaction rate	A	N/A		-99999	
		B	N/A		0	
		C	N/A		0	
		D	N/A		0	

As shown in the rate law for both of the reactions, the adsorption term was the same so, the values were set the same. Table S3 contains the adsorption term parameters used in the model.

Table S4. Adsorption Term Parameters for Reaction Model

	Term	1	2	3	4	5	6	7	8	9
Adsorption constants	A	0	0.05	0.01	0.01	0.01	0.01	0.01	0.01	0.01
	B	0	0.001	0.001	0.001	0.001	0.001	0.001	0.001	0.001
	C	0	0	0	0	0	0	0	0	0
	D	0	0	0	0	0	0	0	0	0

3. Supplementary Fig. S1-4

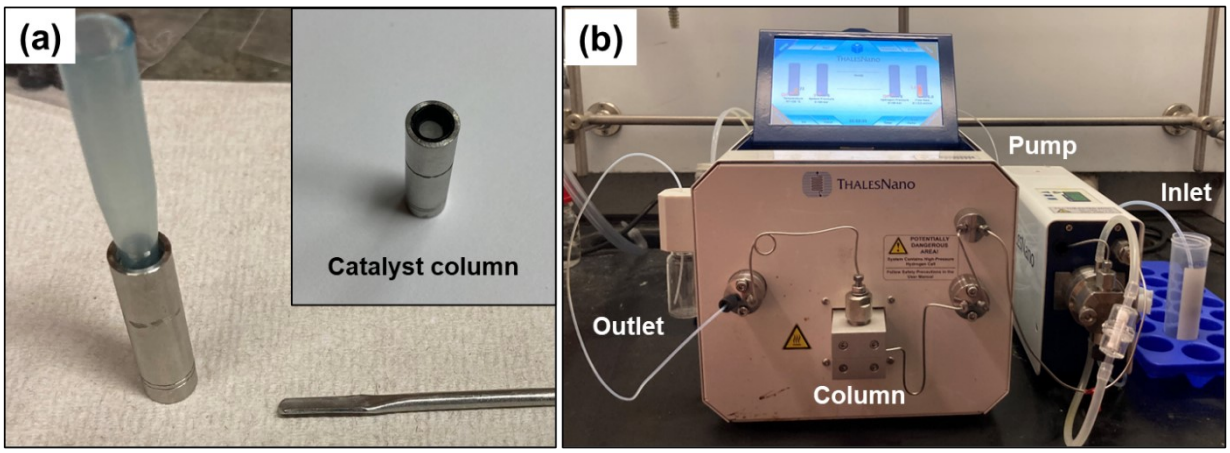

Fig. S1. (a) Image of the catalyst column. (b) Reaction set up.

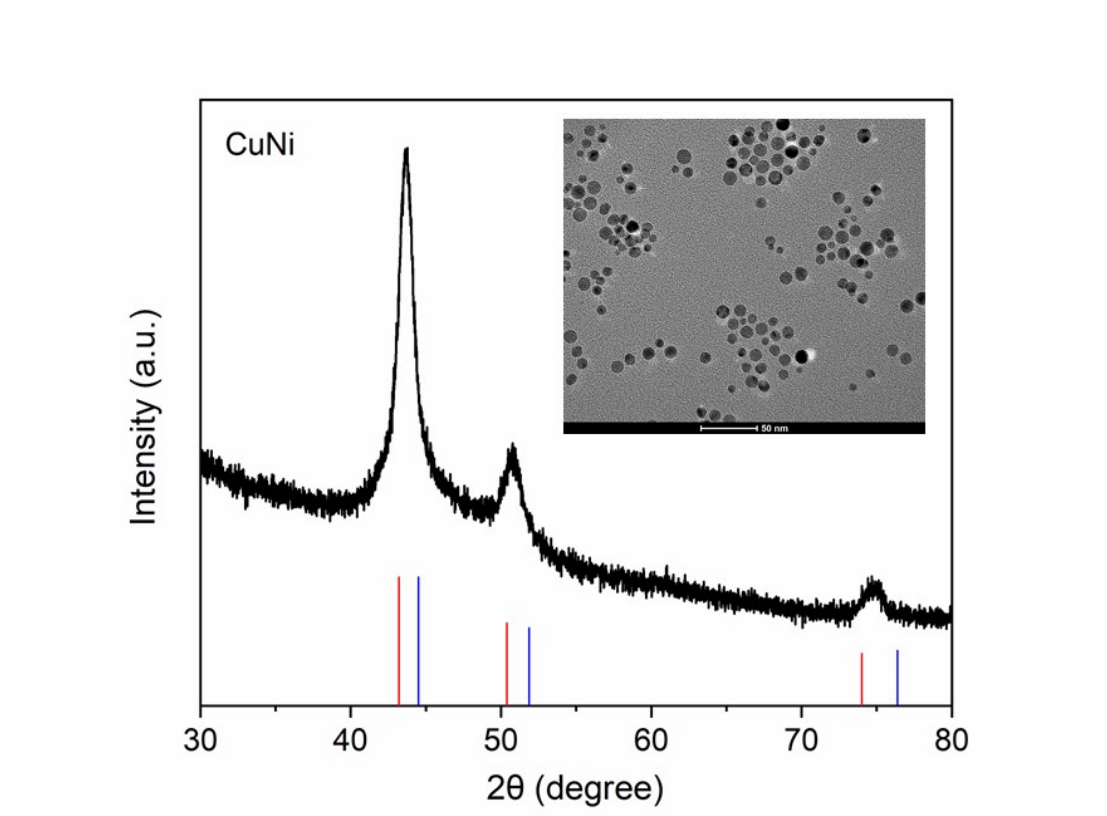

Fig. S2. XRD pattern of CuNi NPs (inset TEM image). Red: Cu (JCPDS 04-0836). Blue: Ni (JCPDS 04-0850).

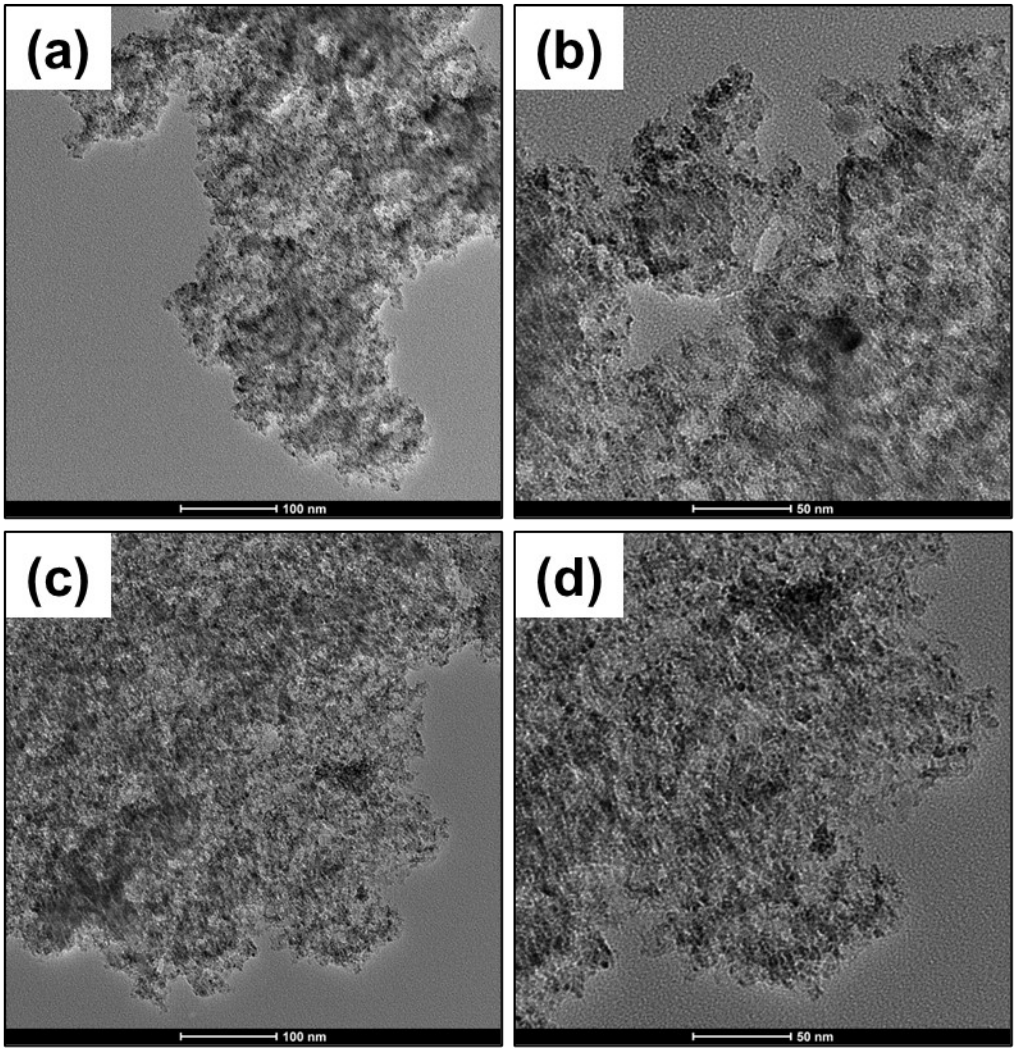

Fig. S3. TEM images of the Pd/C catalyst (a), (b) before, and (c), (d) after the reaction.

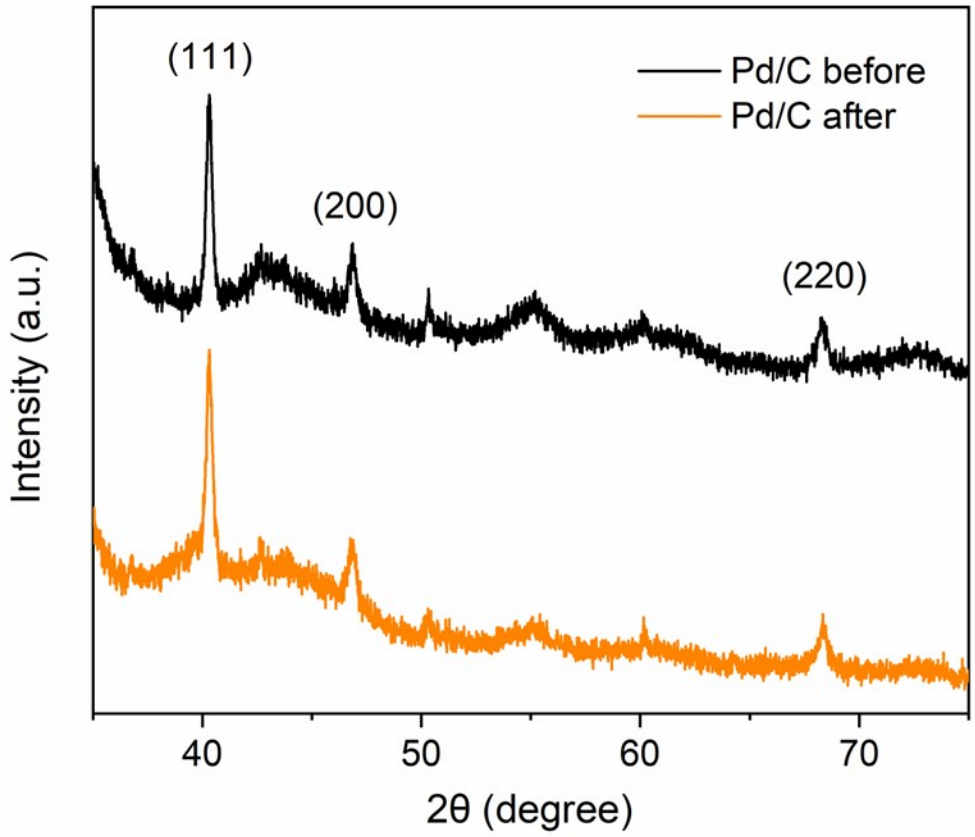

Fig. S4. XRD patterns of the Pd/C catalyst before (top, black) and after (bottom, orange) the reaction.

4. Supplementary Scheme S1

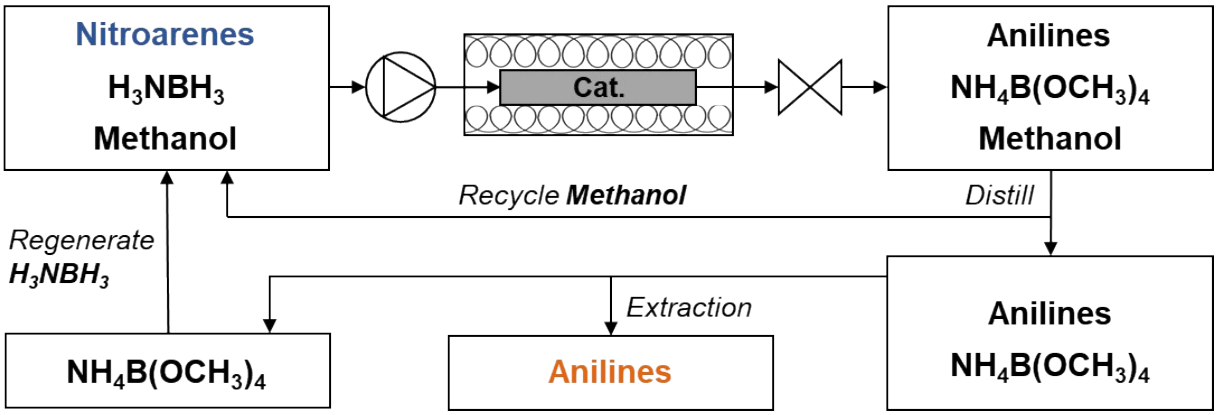

Scheme S1. Illustration of aniline production and AB/solvent recycling.

Product Characterization

After the reaction was completed, an aliquot of the reaction solution (0.5 mL) was collected, the methanol removed under reduced pressure, and the residue dissolved in either $CDCl_3$ or $(CD_3)_2SO$. NMR yields were calculated against 1,3,5-trimethoxybenzene as an internal standard.

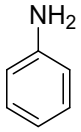

Aniline (1): ^{1}H NMR (400 MHz, $CDCl_3$, 295 K): δ = 7.20-7.16 (m, 2H), 6.80-6.76 (m, 1H), 6.72-6.69 (m, 2H), 3.38 (br, 2H).

$^{13}C\{^1H\}$ NMR (101 MHz, $CDCl_3$, 295 K): δ = 146.2, 129.4, 118.9, 115.4.

^{1}H and $^{13}C\{^1H\}$ spectra agree with a previous report.[S16]

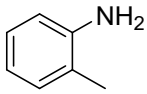

***o*-Toluidine (2)**: ^{1}H NMR (400 MHz, $CDCl_3$, 295 K): δ = 7.09-7.03 (m, 2H), 6.79-6.75 (m, 2H), 2.21 (s, 3H).

$^{13}C\{^1H\}$ NMR (101 MHz, $CDCl_3$, 295 K): δ = 143.3, 130.7, 127.1, 123.4, 119.8, 115.9, 17.5.

^{1}H and $^{13}C\{^1H\}$ spectra agree with a previous report. [S17]

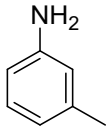

***m*-Toluidine (3)**: ^{1}H NMR (400 MHz, $CDCl_3$, 295 K): δ = 7.09 (t, *J* = 7.6 Hz, 1H), 6.71-6.62 (m, 3H), 2.28 (s, 3H).

$^{13}C\{^{1}H\}$ NMR (101 MHz, $CDCl_3$, 295 K): δ = 143.6, 139.5, 129.4, 121.5, 117.4, 113.8, 21.5.

^{1}H and $^{13}C\{^{1}H\}$ spectra agree with a previous report.[S18]

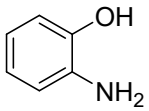

2-Aminophenol (4): ^{1}H NMR (400 MHz, $(CD_3)_2SO$, 295 K): δ = 8.87 (br, 1H), 6.64-6.61 (m, 1H), 6.59-6.50 (m, 2H), 6.41-6.36 (m, 1H), 4.43 (br, 2H).

$^{13}C\{^{1}H\}$ NMR (101 MHz, $(CD_3)_2SO$, 295 K): δ = 143.9, 136.5, 119.4, 116.4, 114.4, 114.3.

^{1}H and $^{13}C\{^{1}H\}$ spectra agree with a previous report. [S19]

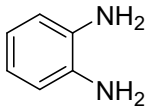

Benzene-1,2-diamine (5): ^{1}H NMR (400 MHz, $(CD_3)_2SO$, 295 K): δ = 6.52-6.47 (m, 2H), 6.39-6.34 (m, 2H), 4.35 (br, 4H).

$^{13}C\{^{1}H\}$ NMR (101 MHz, $(CD_3)_2SO$, 295 K): δ = 134.9, 117.2, 114.5.

^{1}H and $^{13}C\{^{1}H\}$ spectra agree with a previous report.[S20]

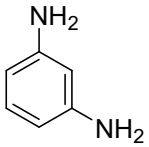

Benzene-1,3-diamine (6): ^{1}H NMR (400 MHz, $(CD_3)_2SO$, 295 K): δ = 6.66-6.63 (m, 1H), 5.82-5.76 (m, 3H), 4.61 (br, 4H).

$^{13}C\{^{1}H\}$ NMR (101 MHz, $(CD_3)_2SO$, 295 K): δ = 149.0, 129.0, 103.0, 100.0.

^{1}H and $^{13}C\{^{1}H\}$ spectra agree with a previous report.[S18]

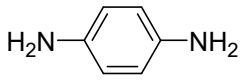

Benzene-1,4-diamine (7): ^{1}H NMR (400 MHz, $(CD_3)_2SO$, 295 K): δ = 6.35 (s, 4H), 4.14 (br, 4H).

$^{13}C\{^{1}H\}$ NMR (101 MHz, $(CD_3)_2SO$, 295 K): δ = 138.9, 115.4.

^{1}H and $^{13}C\{^{1}H\}$ spectra agree with a previous report.[S20]

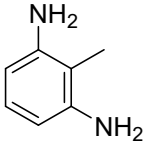

2,6-Diaminotoluene (8): ^{1}H NMR (400 MHz, $(CD_3)_2SO$, 295 K): δ = 6.56 (t, *J* = 7.9 Hz, 1H), 5.93 (d, *J* = 7.8 Hz, 2H), 4.44 (br, 4H), 1.80 (s, 3H).

$^{13}C\{^{1}H\}$ NMR (101 MHz, $(CD_3)_2SO$, 295 K): δ = 146.6, 125.7, 104.1, 10.2.

^{1}H and $^{13}C\{^{1}H\}$ spectra agree with a previous report.[S21]

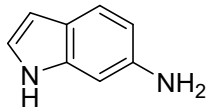

6-Aminoindole (9): ^{1}H NMR (400 MHz, $(CD_3)_2SO$, 295 K): δ = 10.41 (br, 1H), 7.18-7.14 (m, 1H), 6.96-6.93 (m, 1H), 6.56-6.54 (m, 1H), 6.37 (dd, *J* = 8.3, 2.0 Hz, 1H), 6.18-6.15 (m, 1H), 4.63 (br, 2H).

$^{13}C\{^{1}H\}$ NMR (101 MHz, $(CD_3)_2SO$, 295 K): δ = 143.6, 137.5, 121.7, 120.0, 119.5, 109.8, 100.8, 95.2.

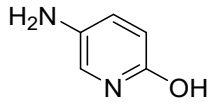

5-Aminopyridin-2-ol (10): ^{1}H NMR (400 MHz, $(CD_3)_2SO$, 295 K): δ = 7.04 (dd, *J* = 9.3, 3.1 Hz, 1H), 6.76-6.74 (m, 1H), 6.21 (dd, *J* = 9.4, 0.6 Hz, 1H), 4.23 (br, 2H).

$^{13}C\{^{1}H\}$ NMR (101 MHz, $(CD_3)_2SO$, 295 K): δ = 158.7, 133.9, 130.7, 118.9, 117.8.

NMR Spectra

^{1}H NMR: Aniline (1)

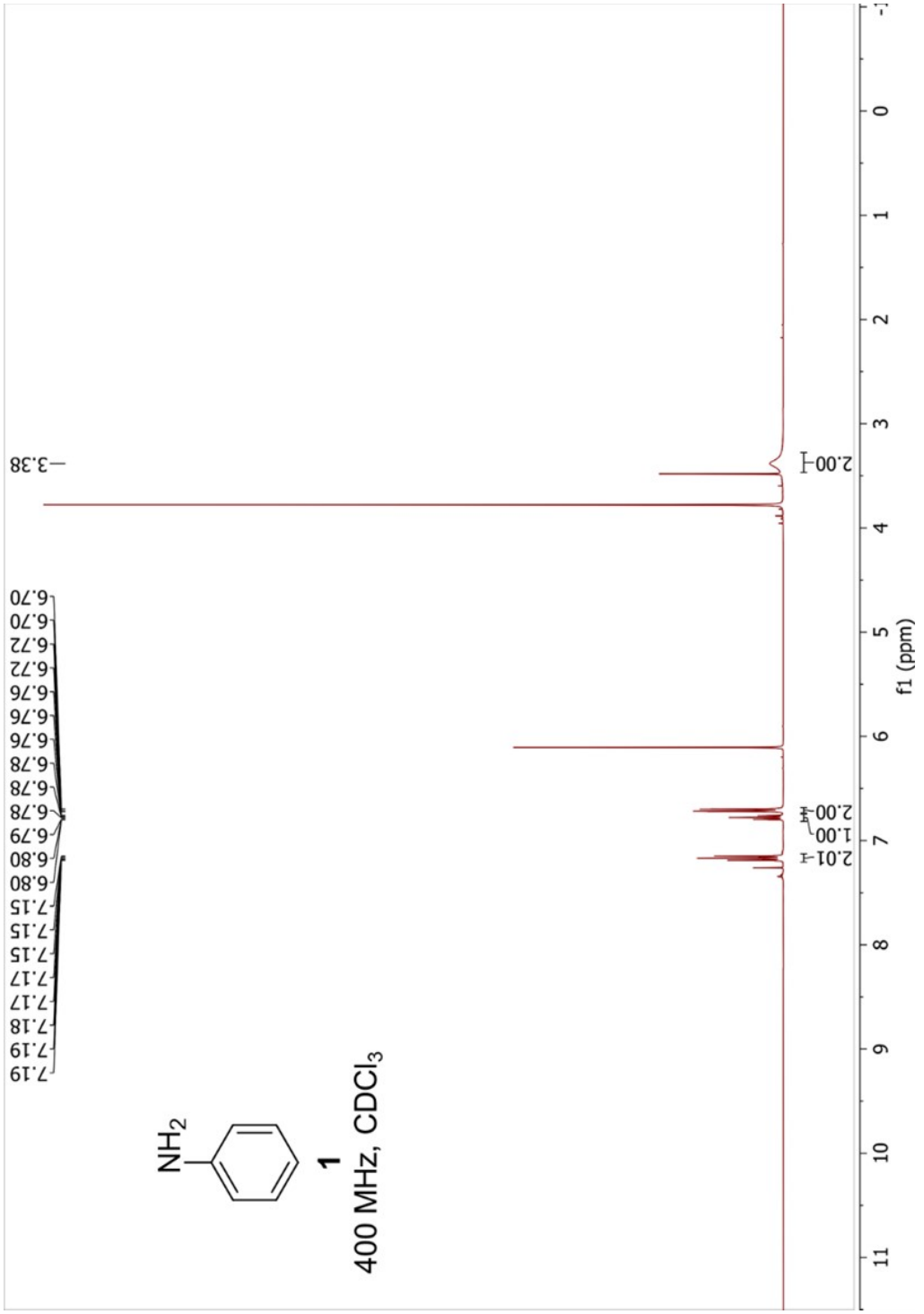

$^{13}C\{^{1}H\}$ NMR: Aniline (1)

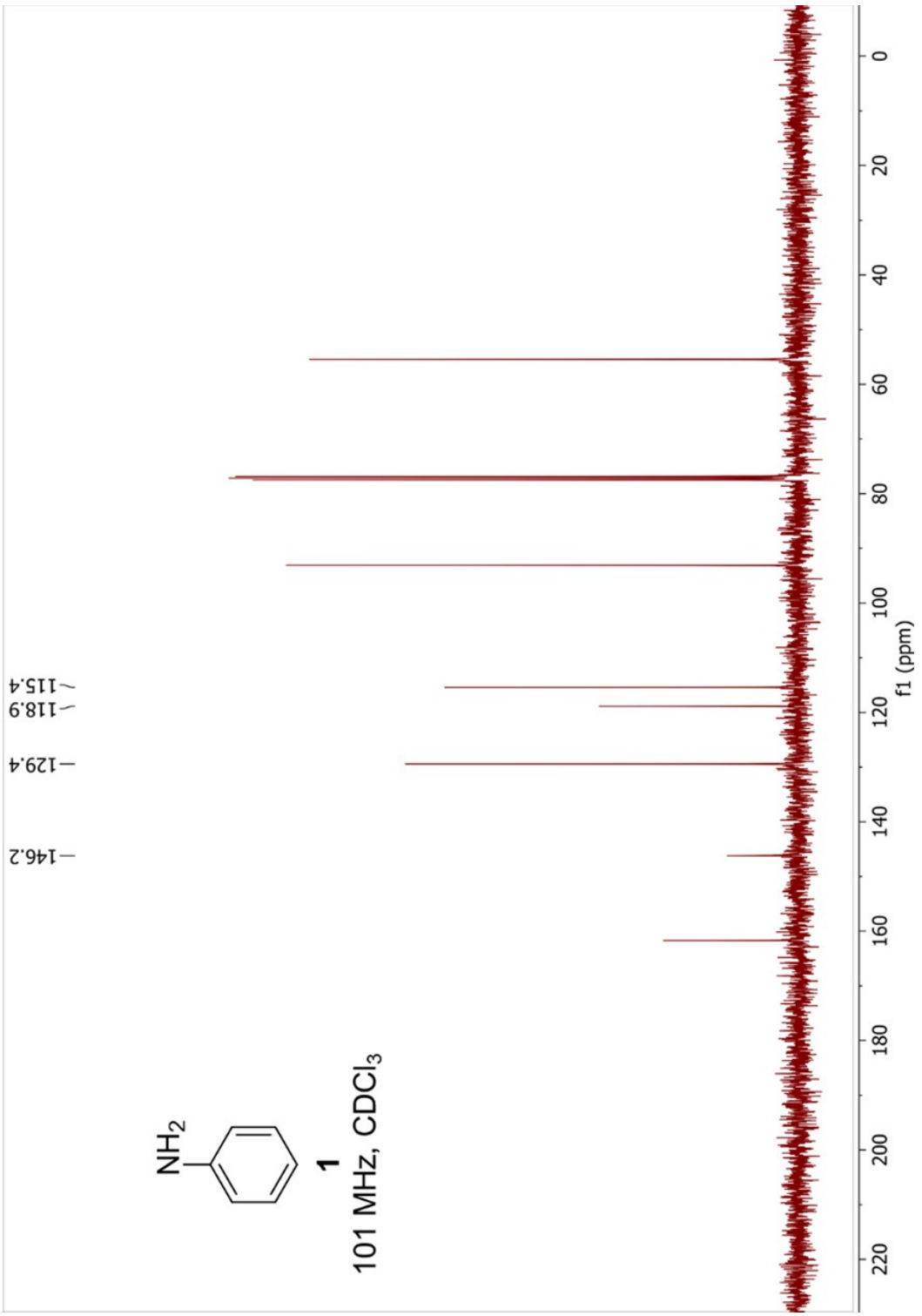

^{1}H NMR: *o*-Toluidine (2)

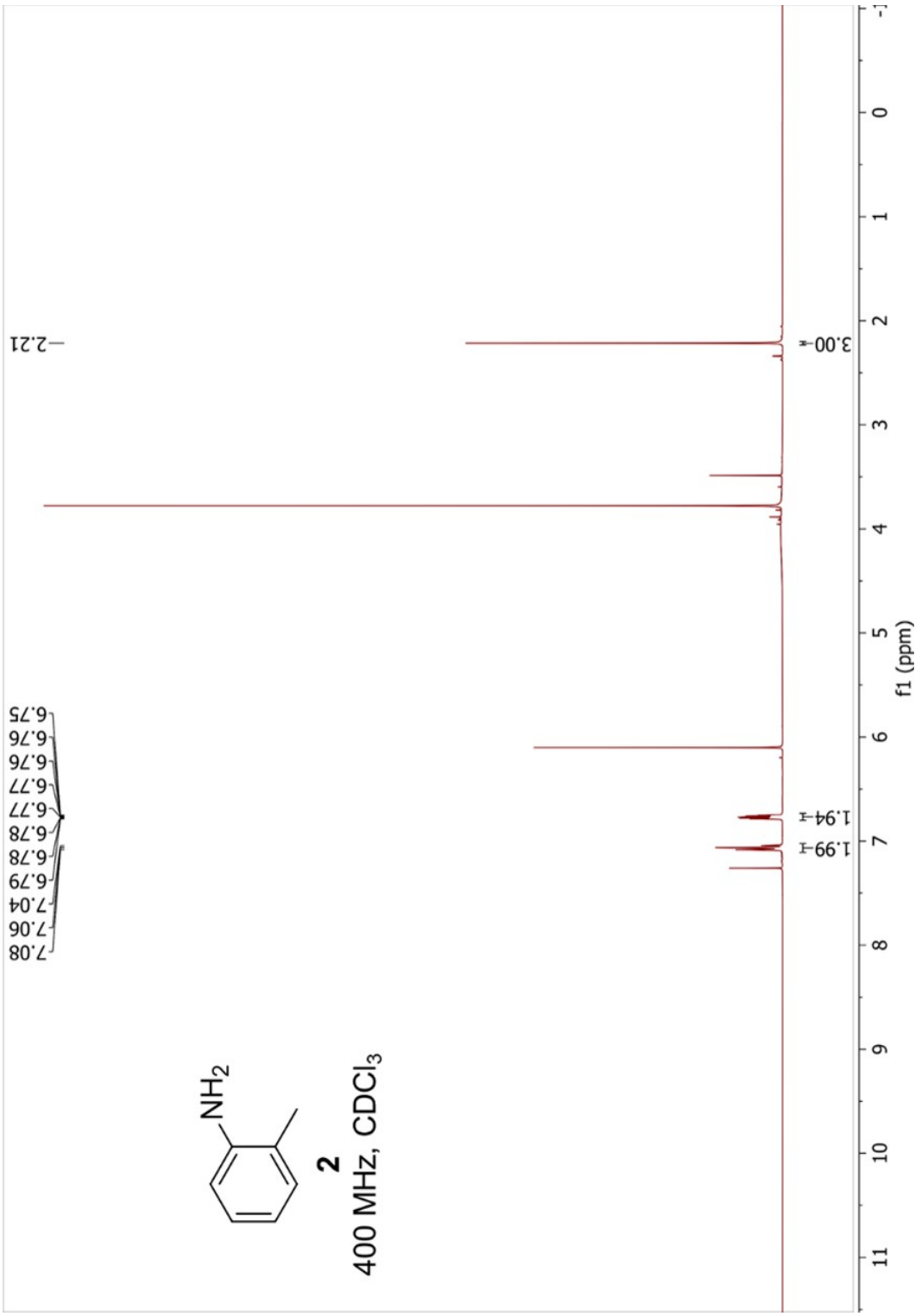

$^{13}C\{^{1}H\}$ NMR: *o*-Toluidine (2)

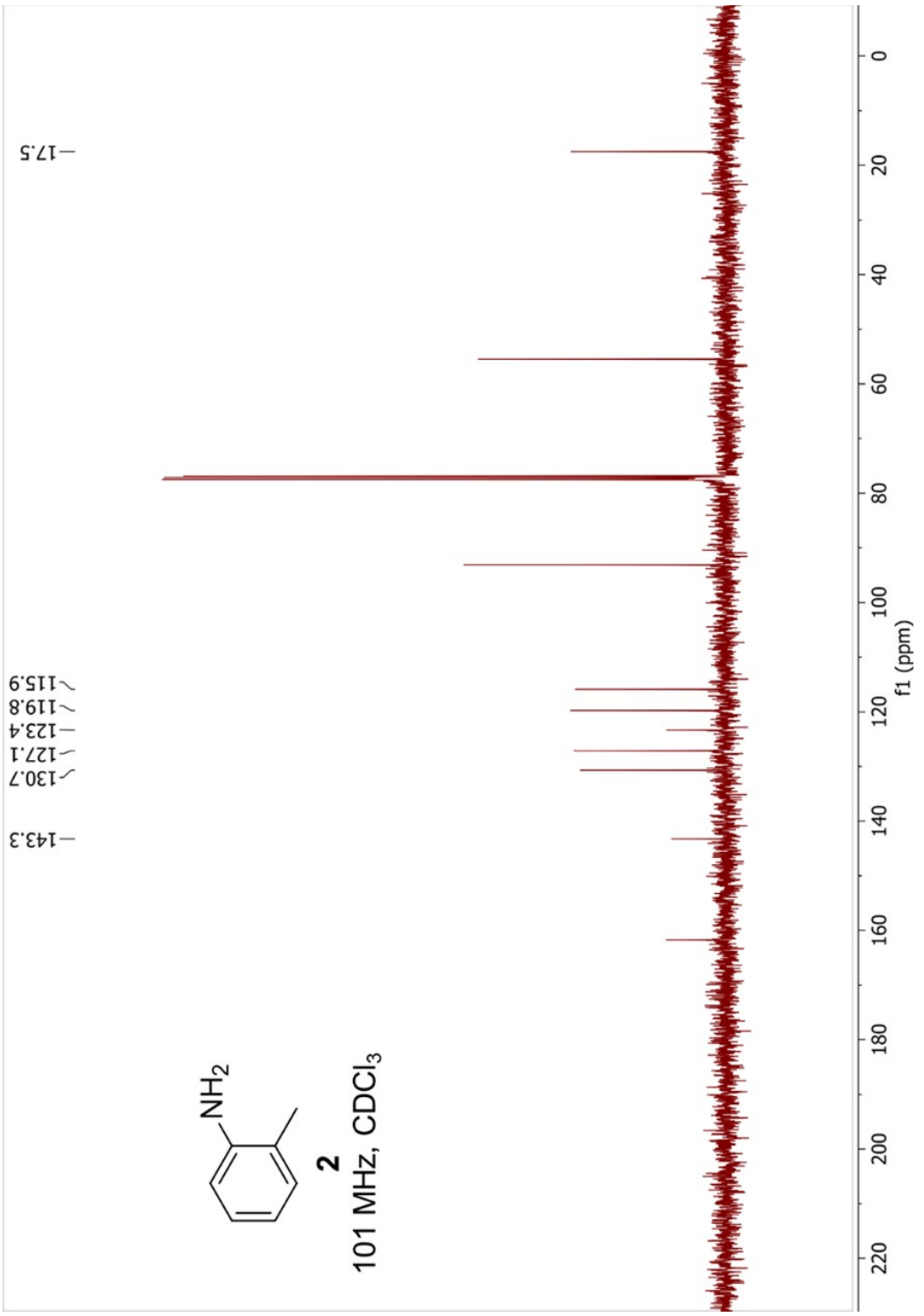

^{1}H NMR: *m*-Toluidine (3)

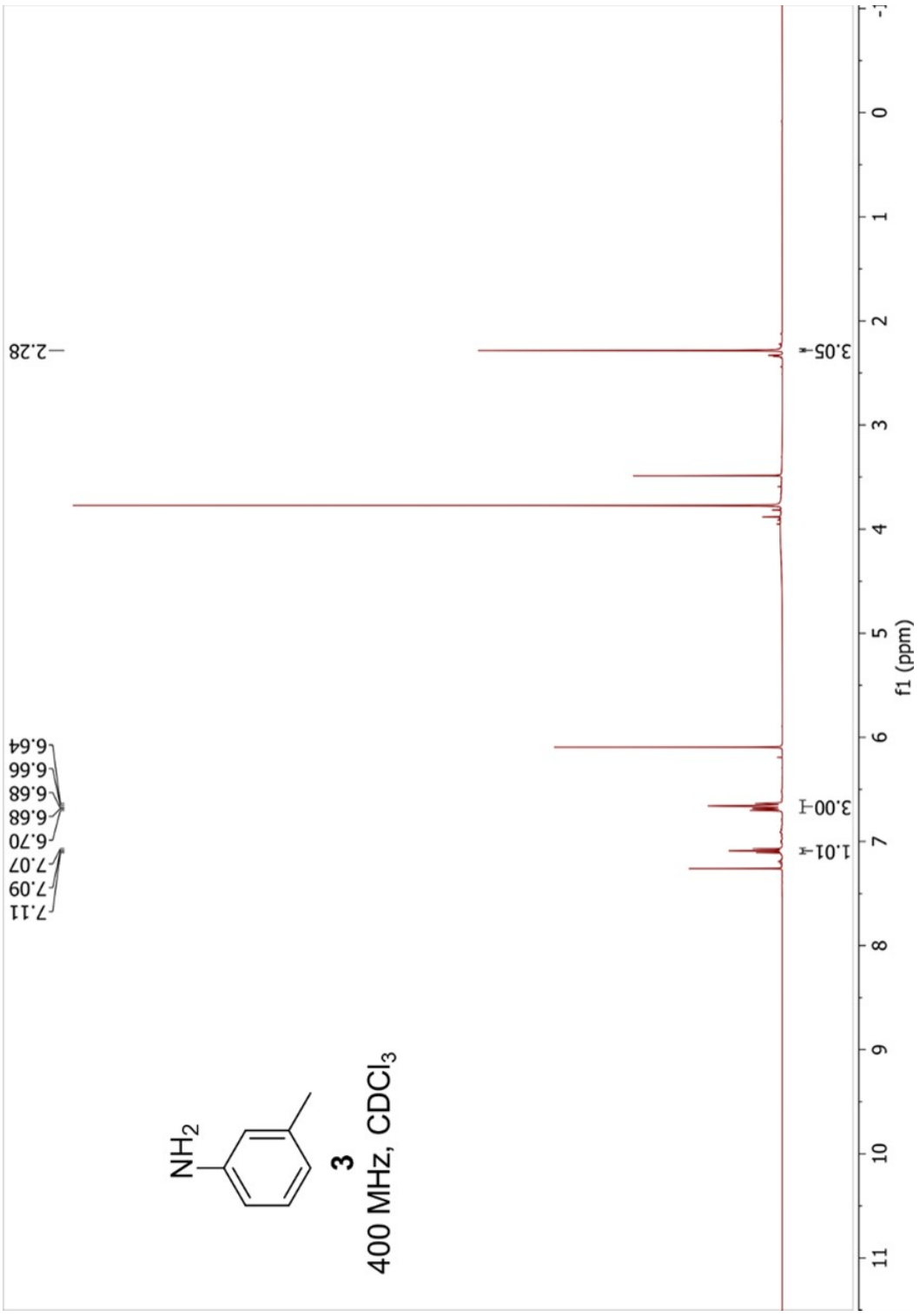

$^{13}C\{^{1}H\}$ NMR: *m*-Toluidine (3)

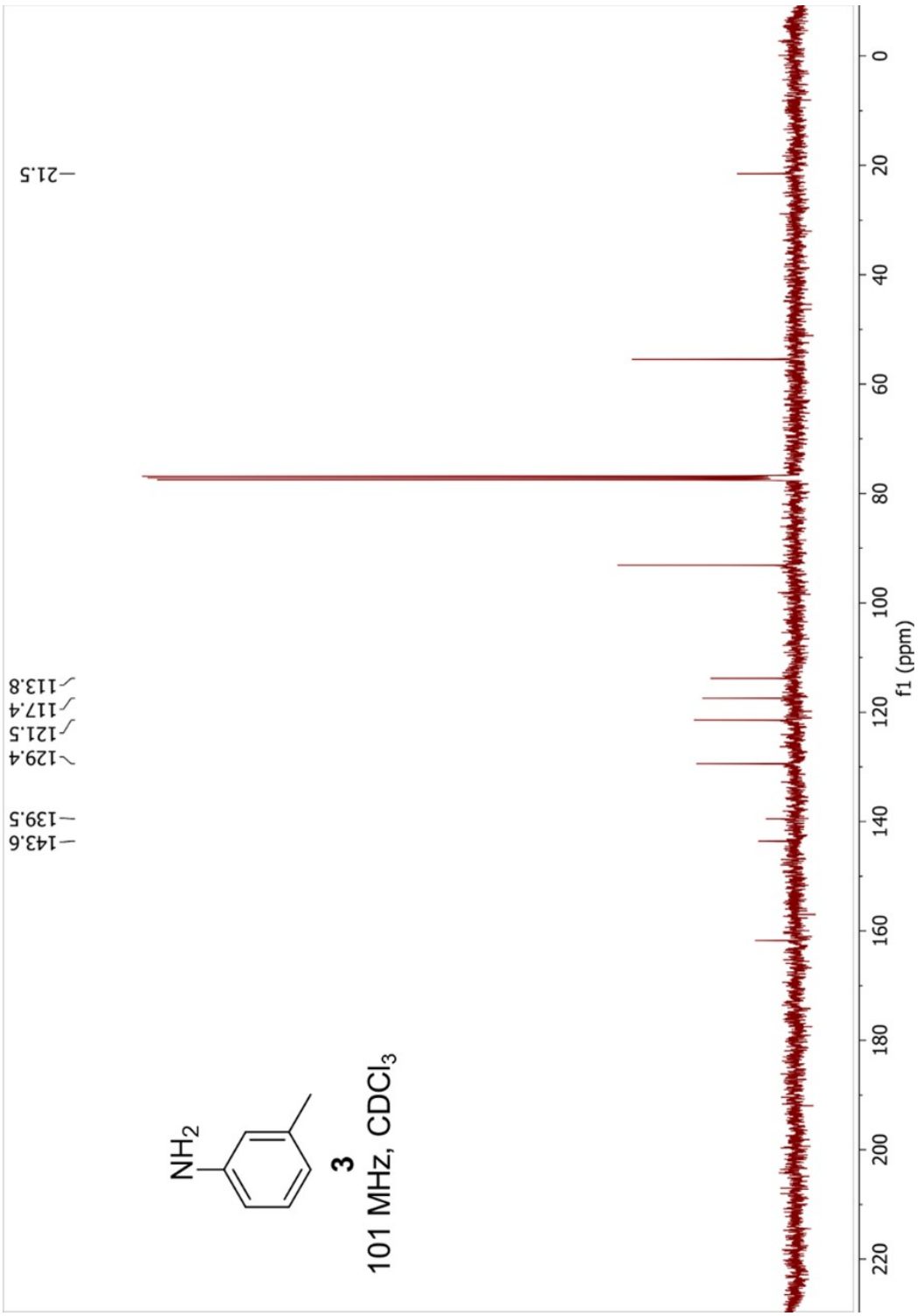

^{1}H NMR: 2-Aminophenol (4)

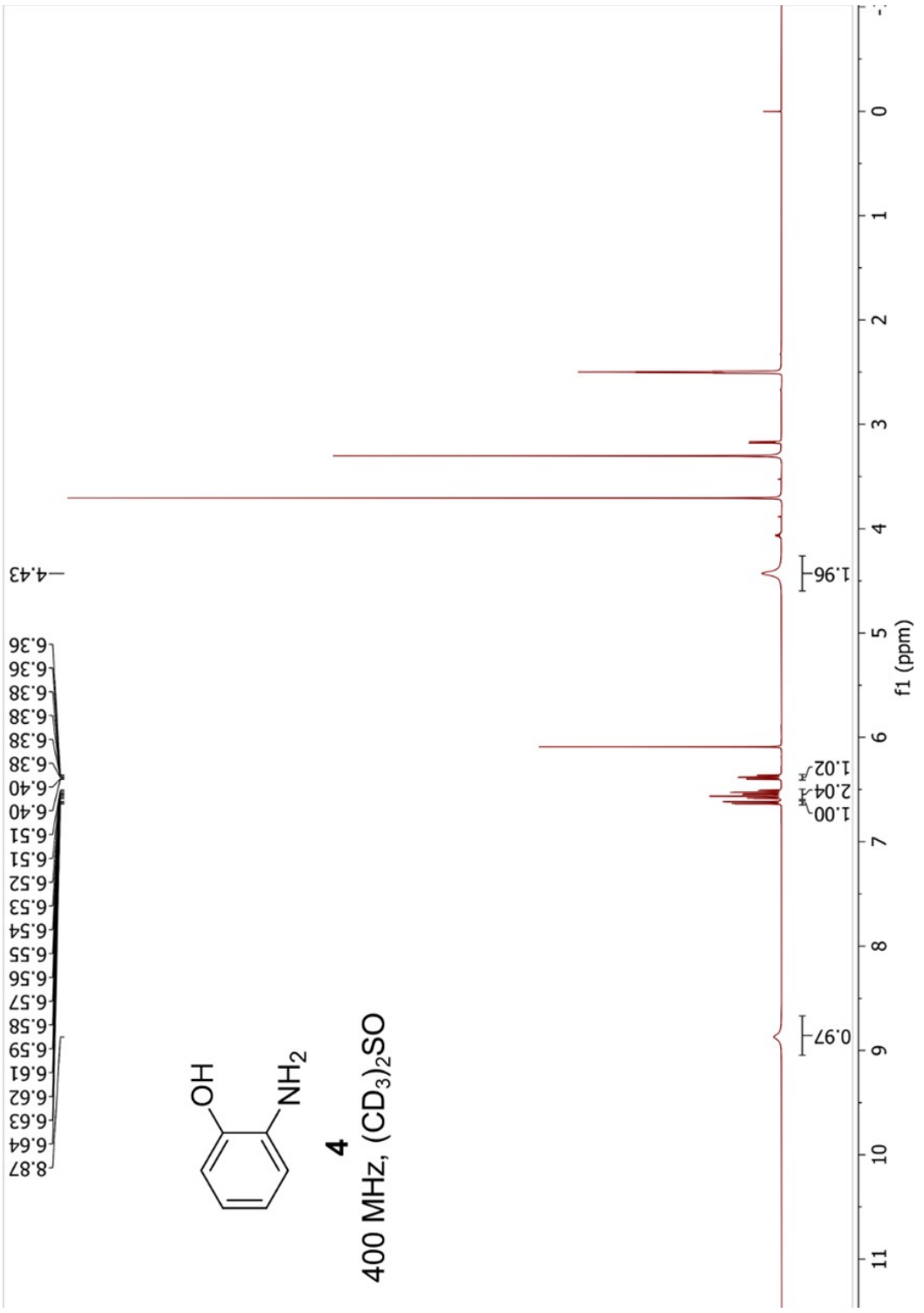

$^{13}C\{^{1}H\}$ NMR: 2-Aminophenol (4)

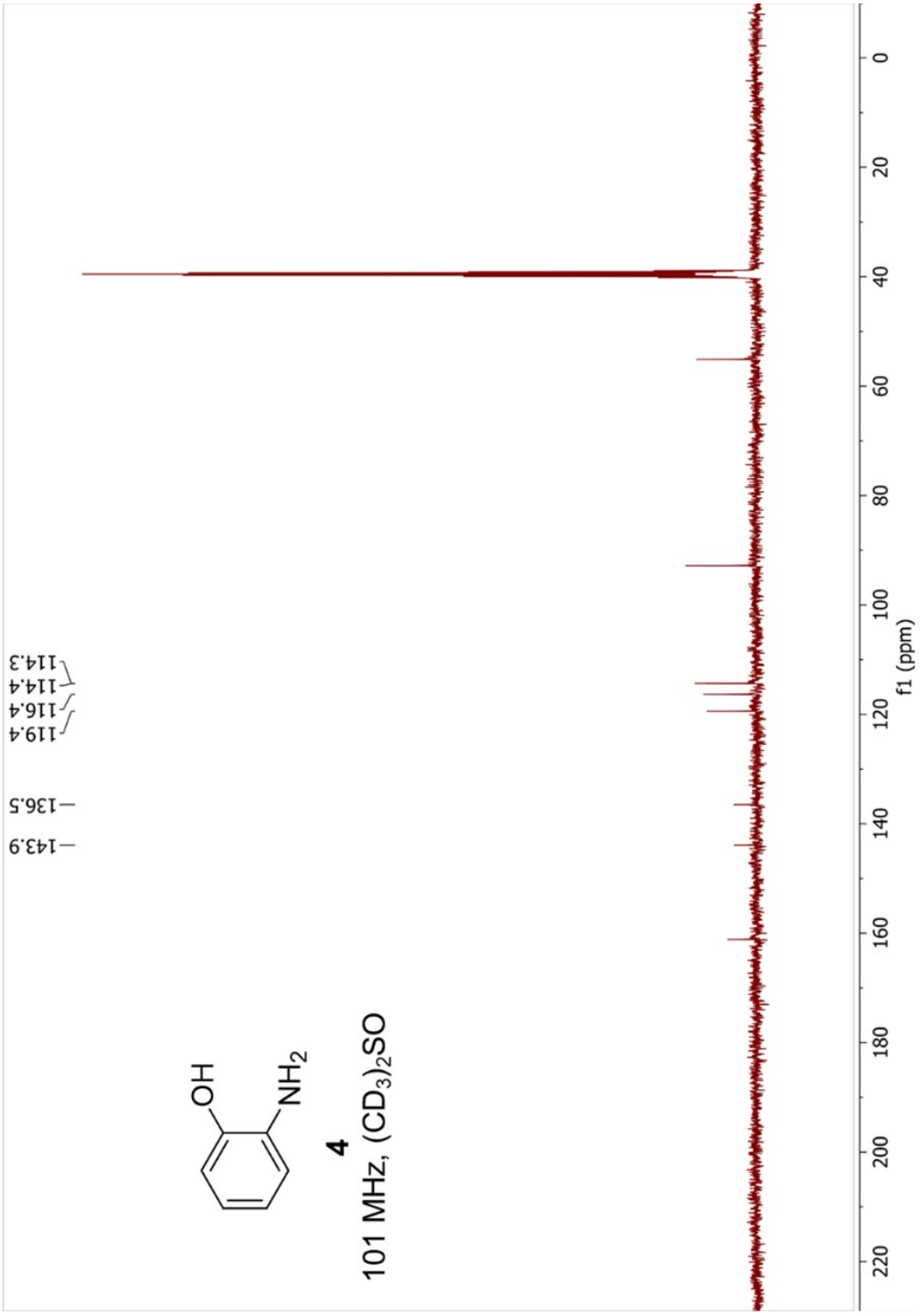

^{1}H NMR: Benzene-1,2-diamine (5)

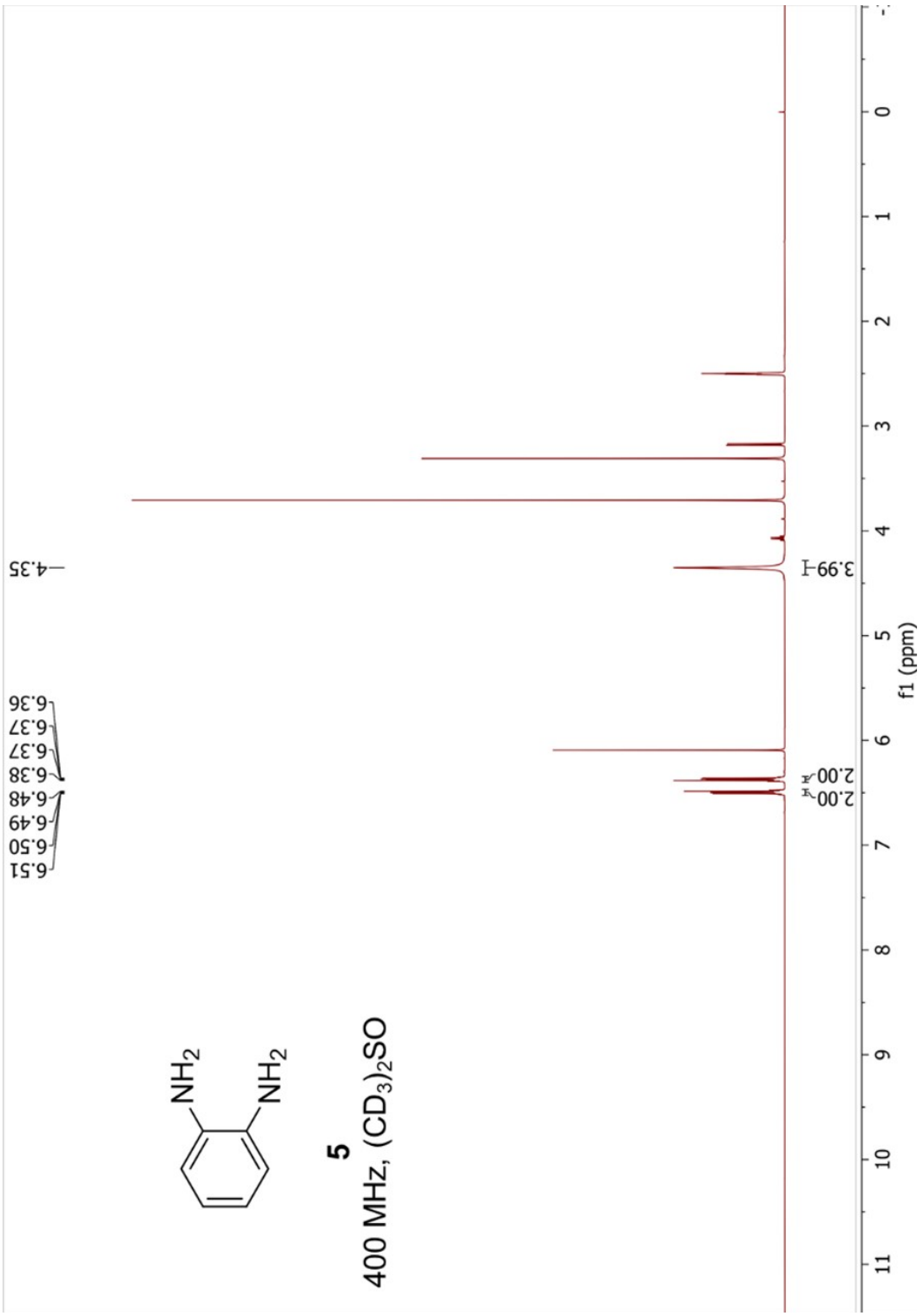

$^{13}C\{^{1}H\}$ NMR: Benzene-1,2-diamine (5)

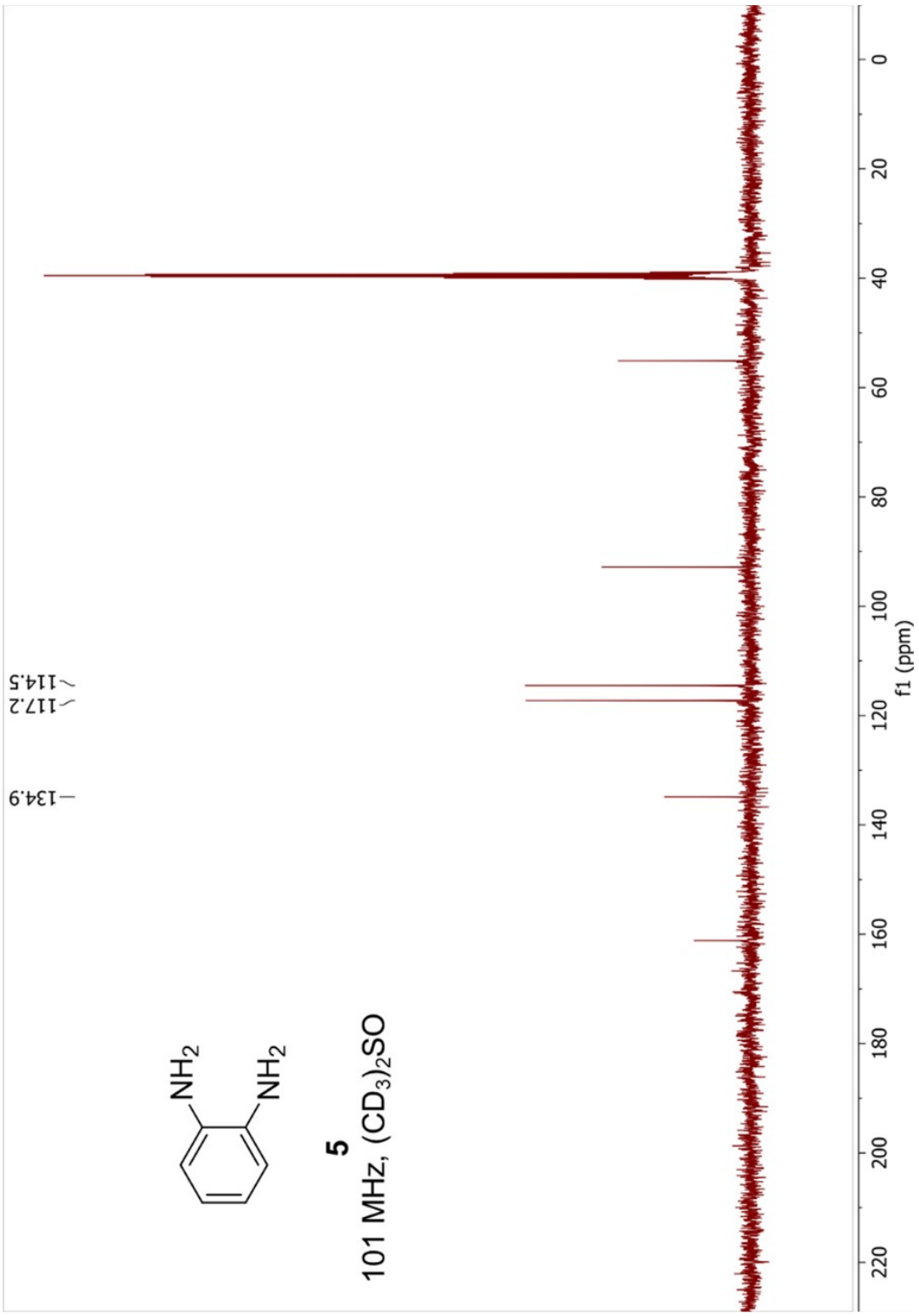

^{1}H NMR: Benzene-1,3-diamine (6)

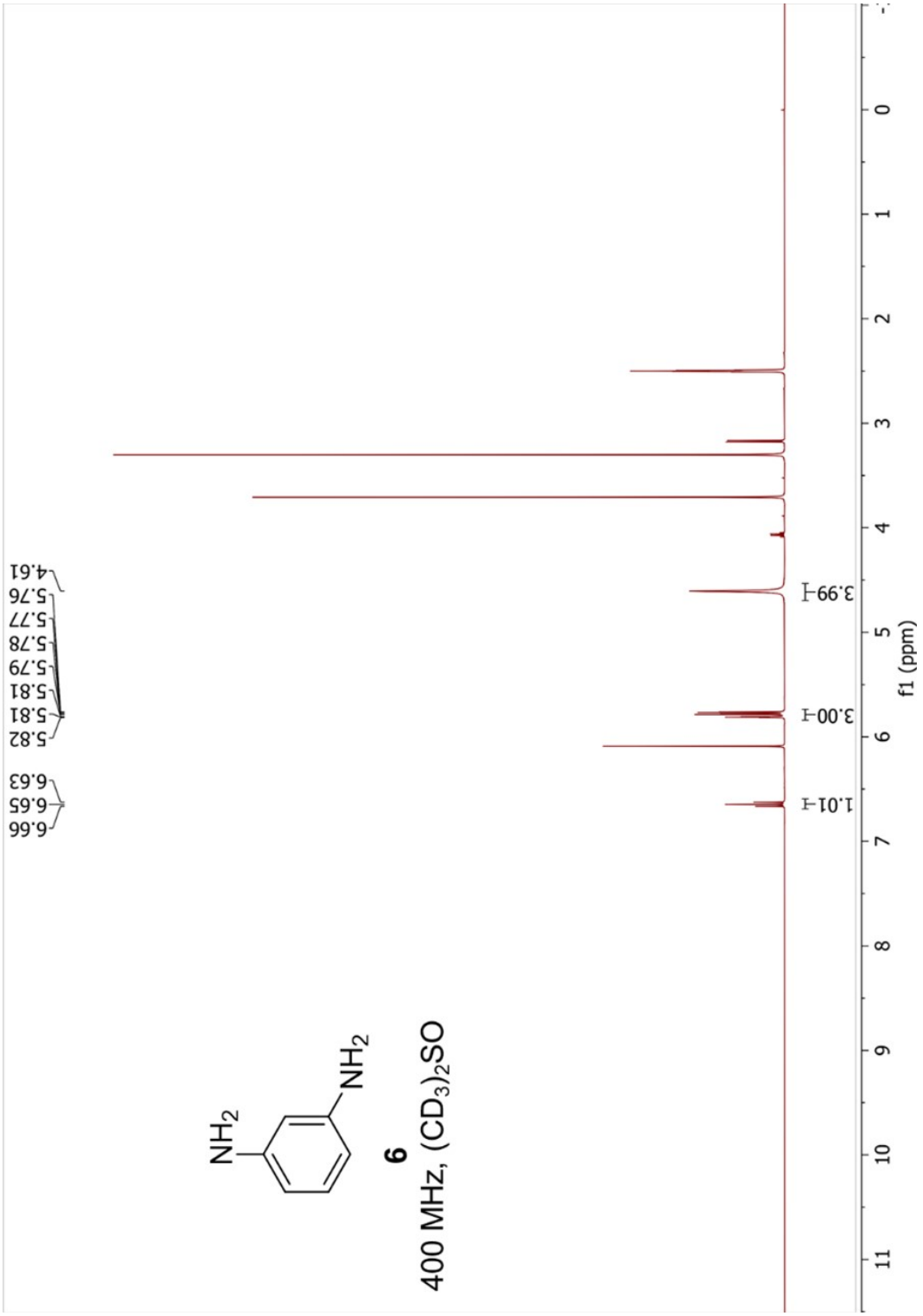

$^{13}C\{^{1}H\}$ NMR: Benzene-1,3-diamine (6)

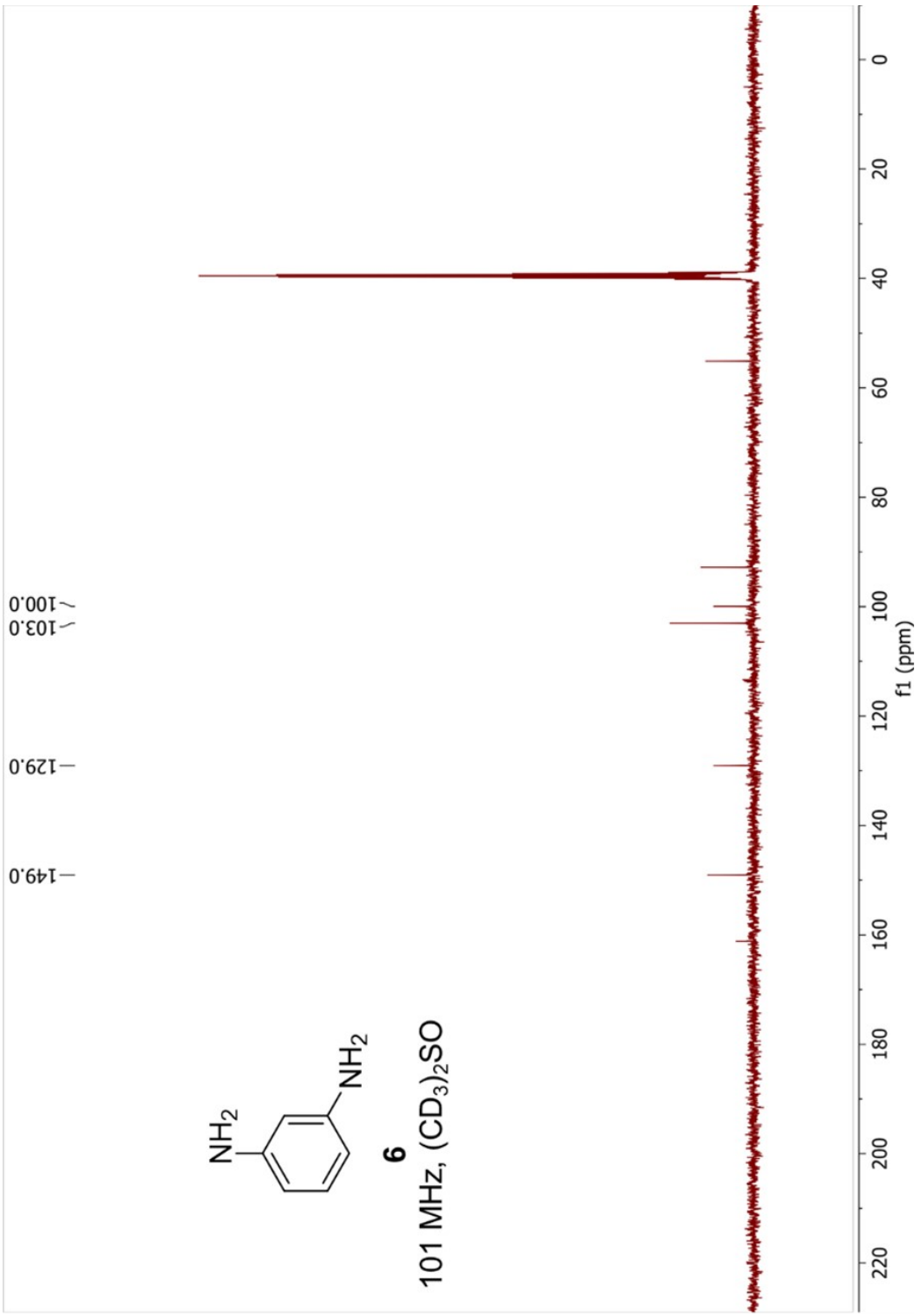

^{1}H NMR: Benzene-1,4-diamine (7)

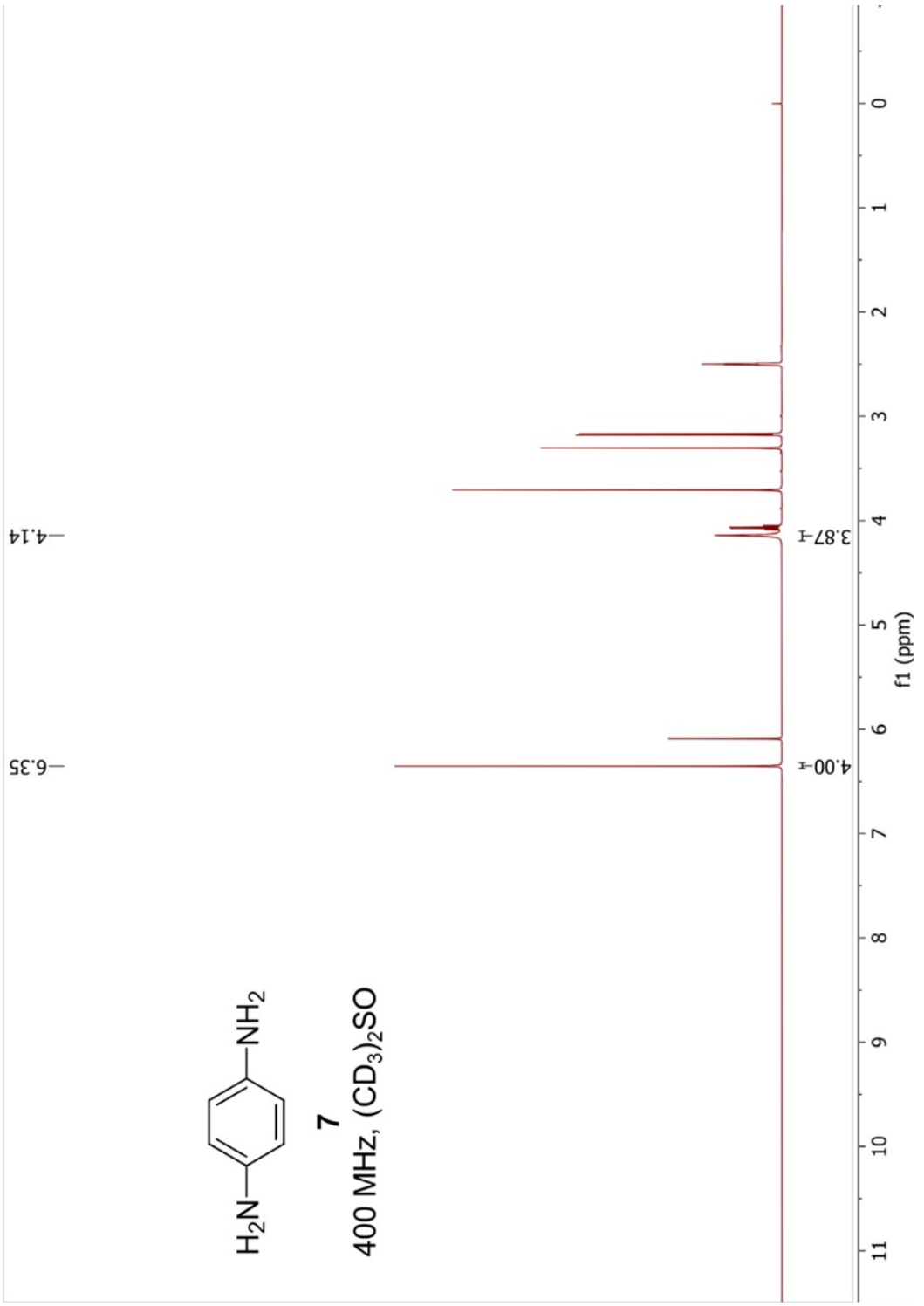

$^{13}C\{^{1}H\}$ NMR: Benzene-1,4-diamine (7)

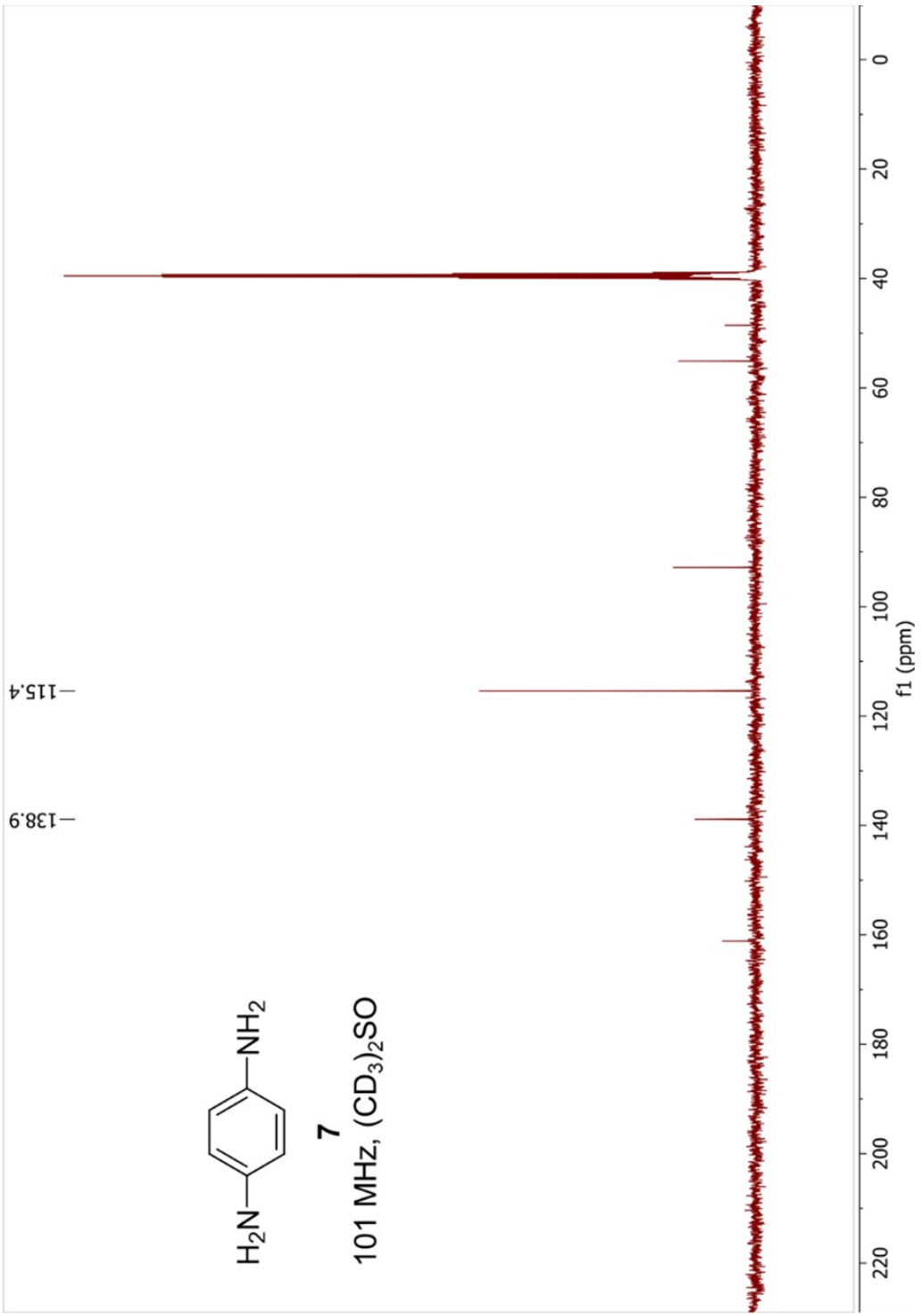

^{1}H NMR: 2,6-Diaminotoluene (8)

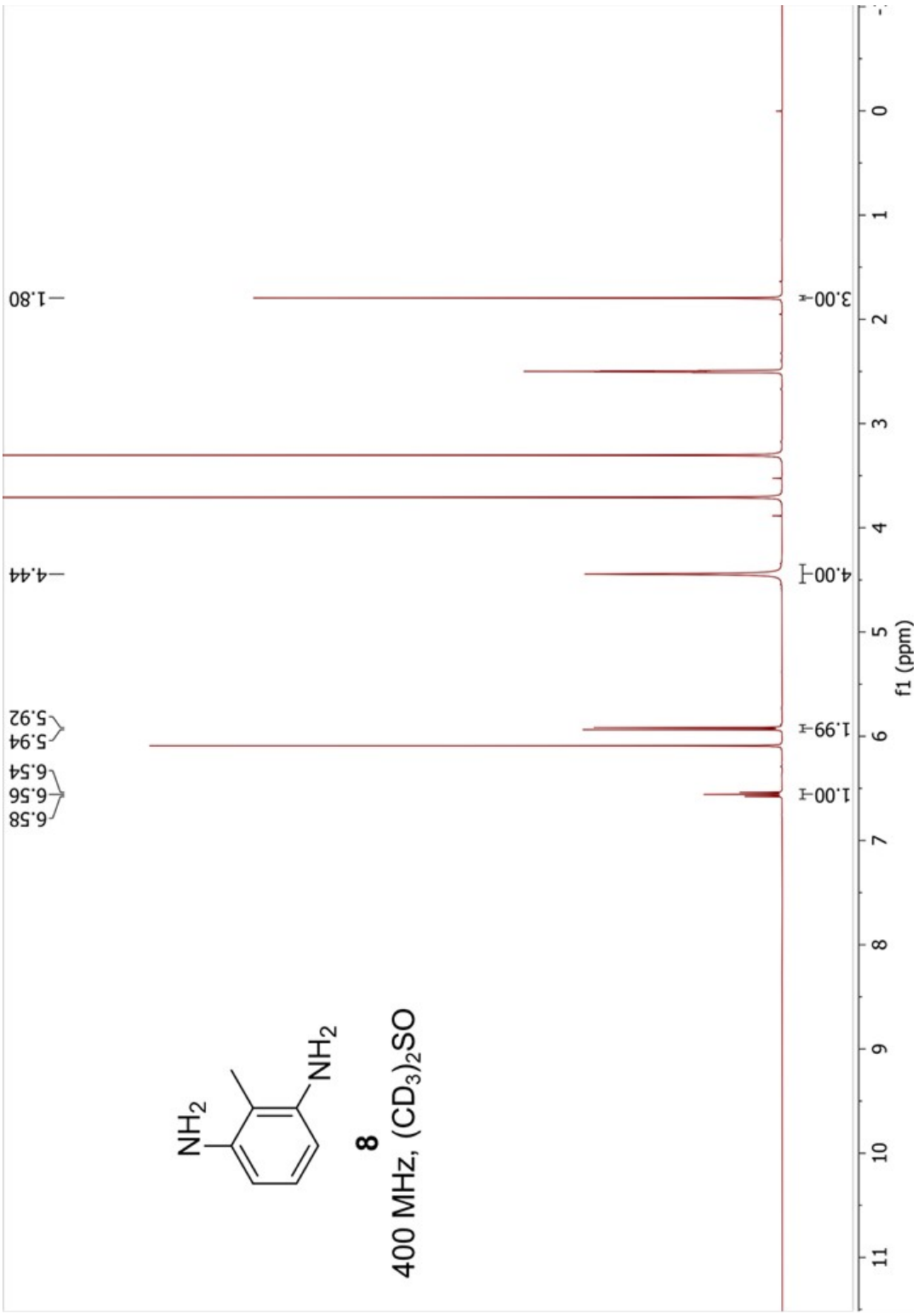

$^{13}C\{^{1}H\}$ NMR: 2,6-Diaminotoluene (8)

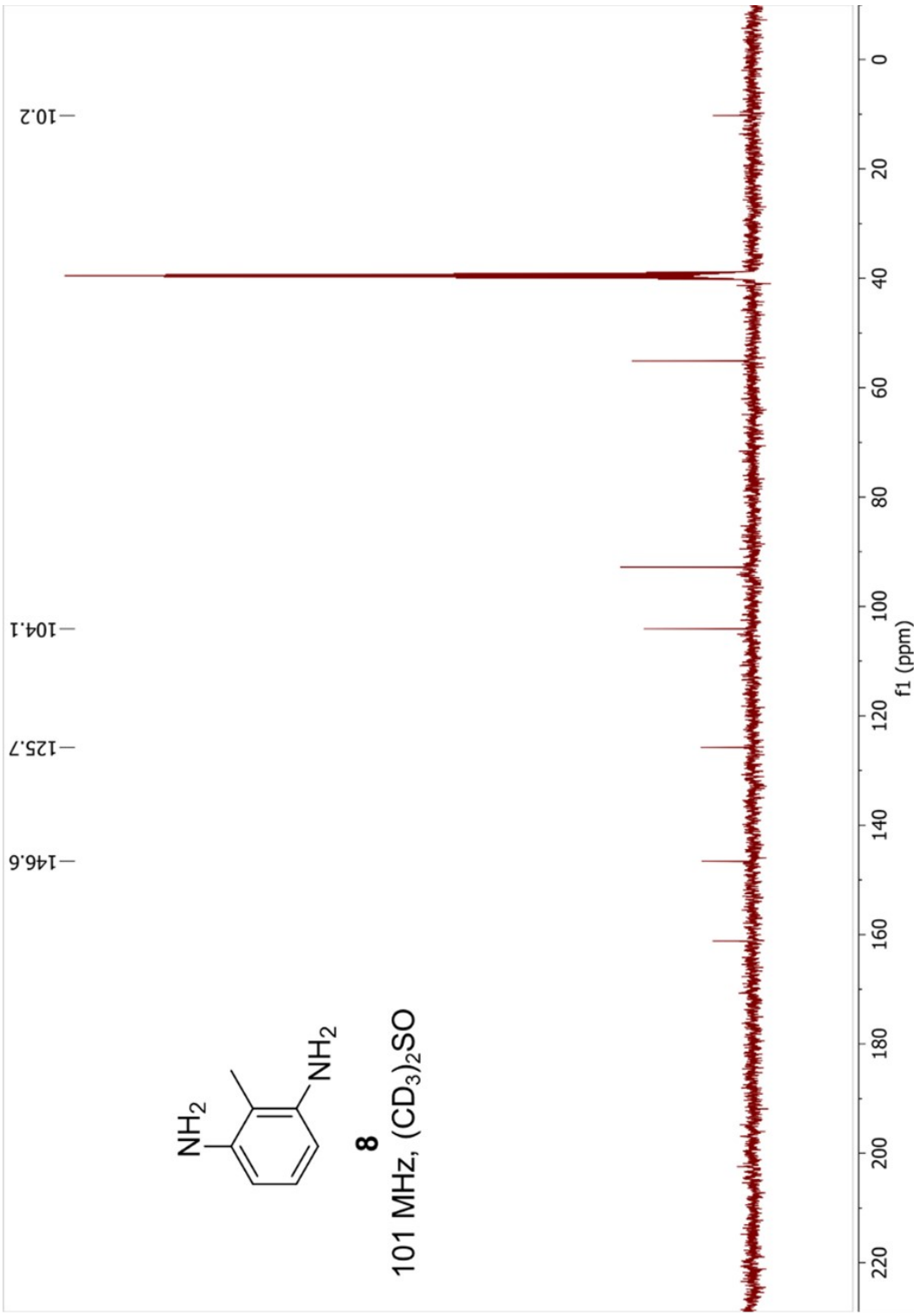

^{1}H NMR: 6-Aminoindole (9)

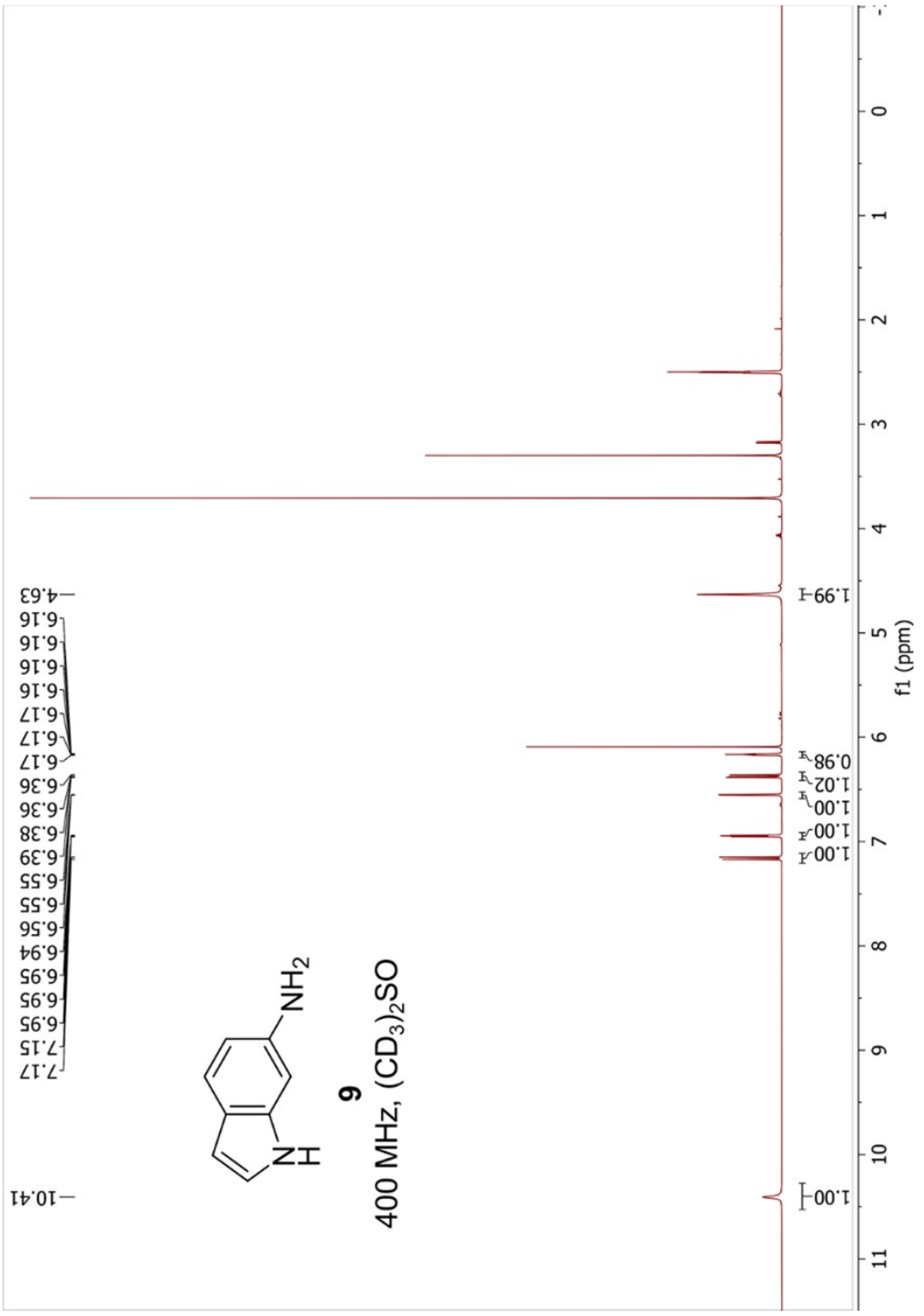

$^{13}C\{^{1}H\}$ NMR: 6-Aminoindole (9)

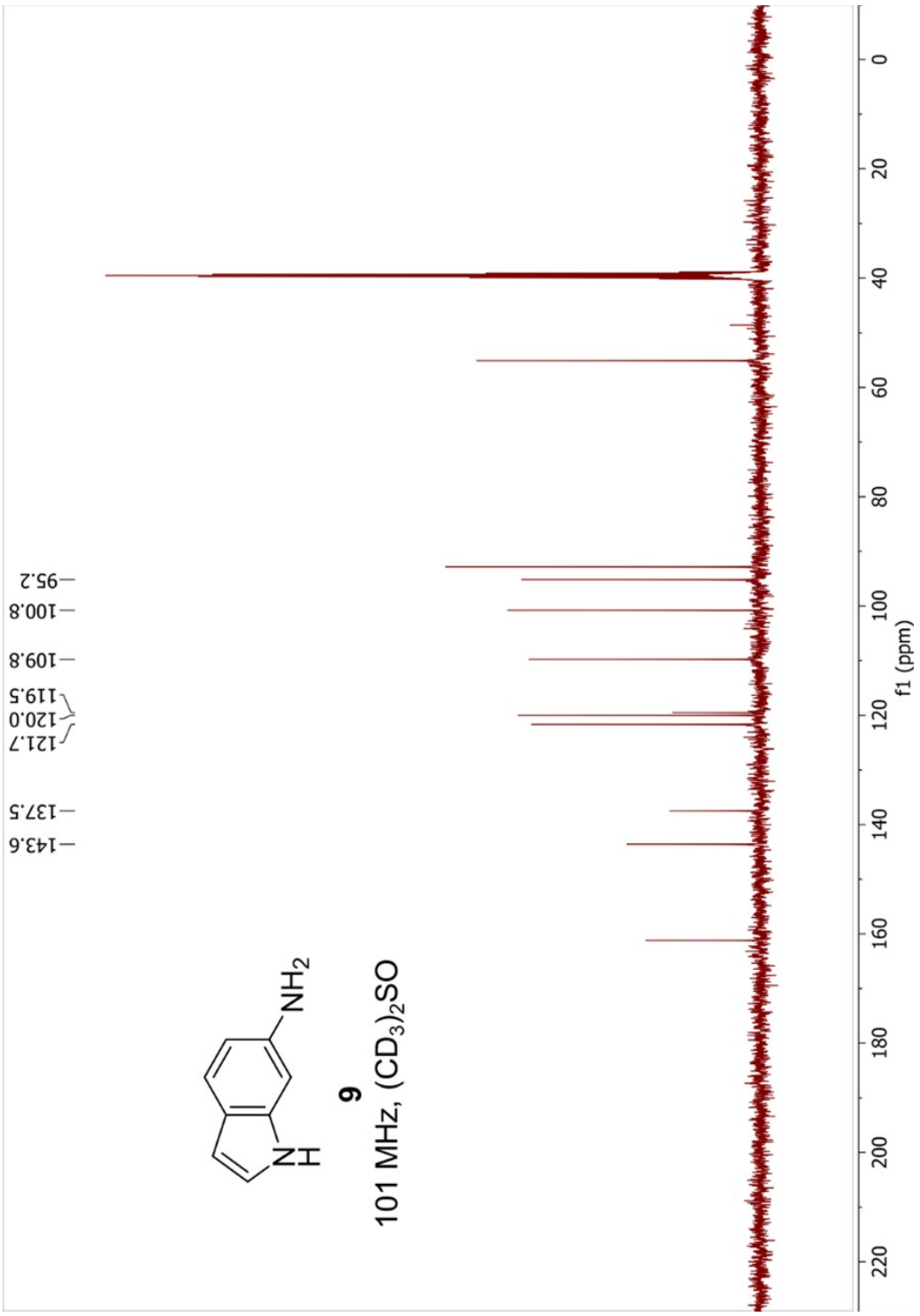

^{1}H NMR: 5-Aminopyridin-2-ol (10)

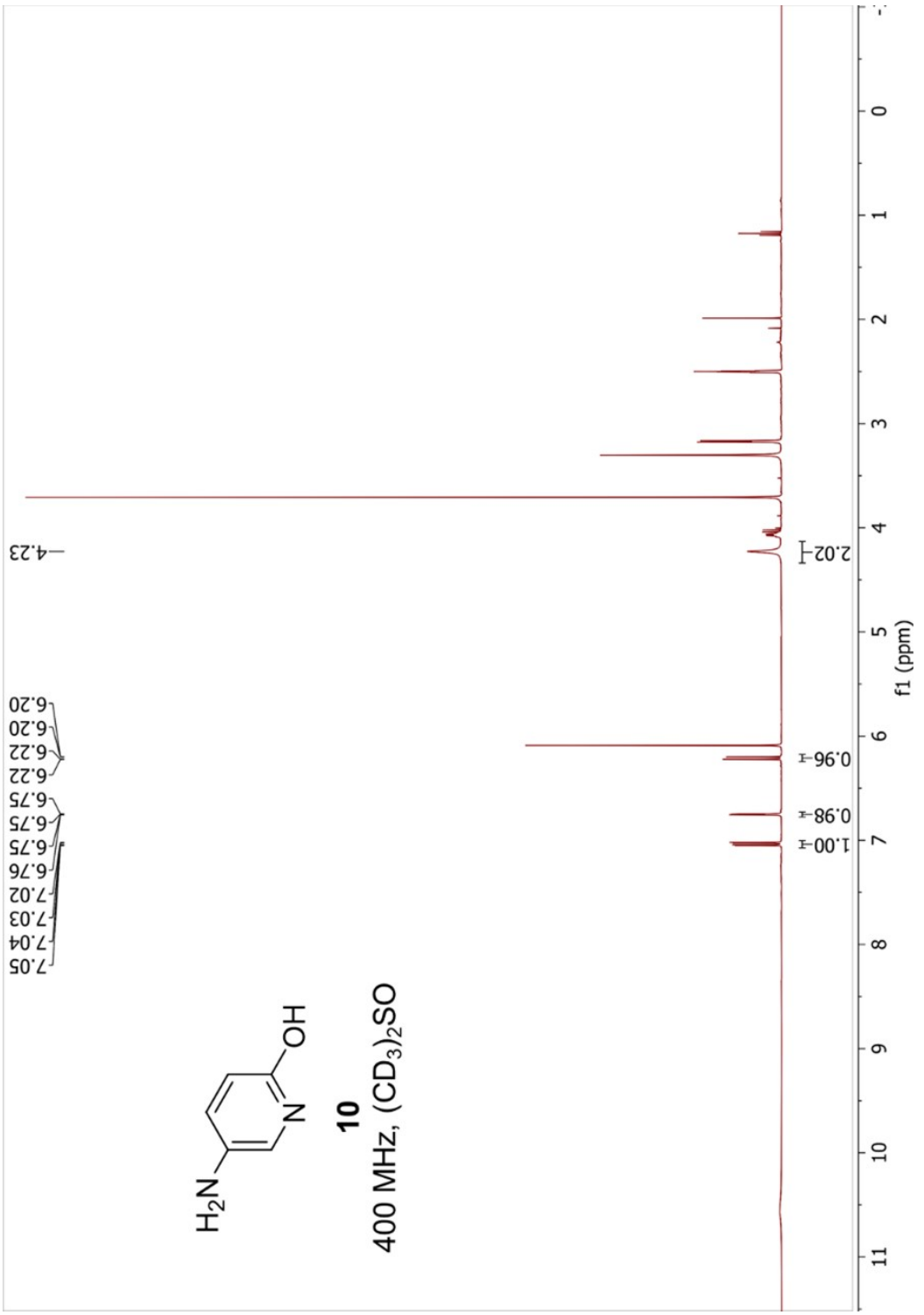

$^{13}C\{^{1}H\}$ NMR: 5-Aminopyridin-2-ol (10)

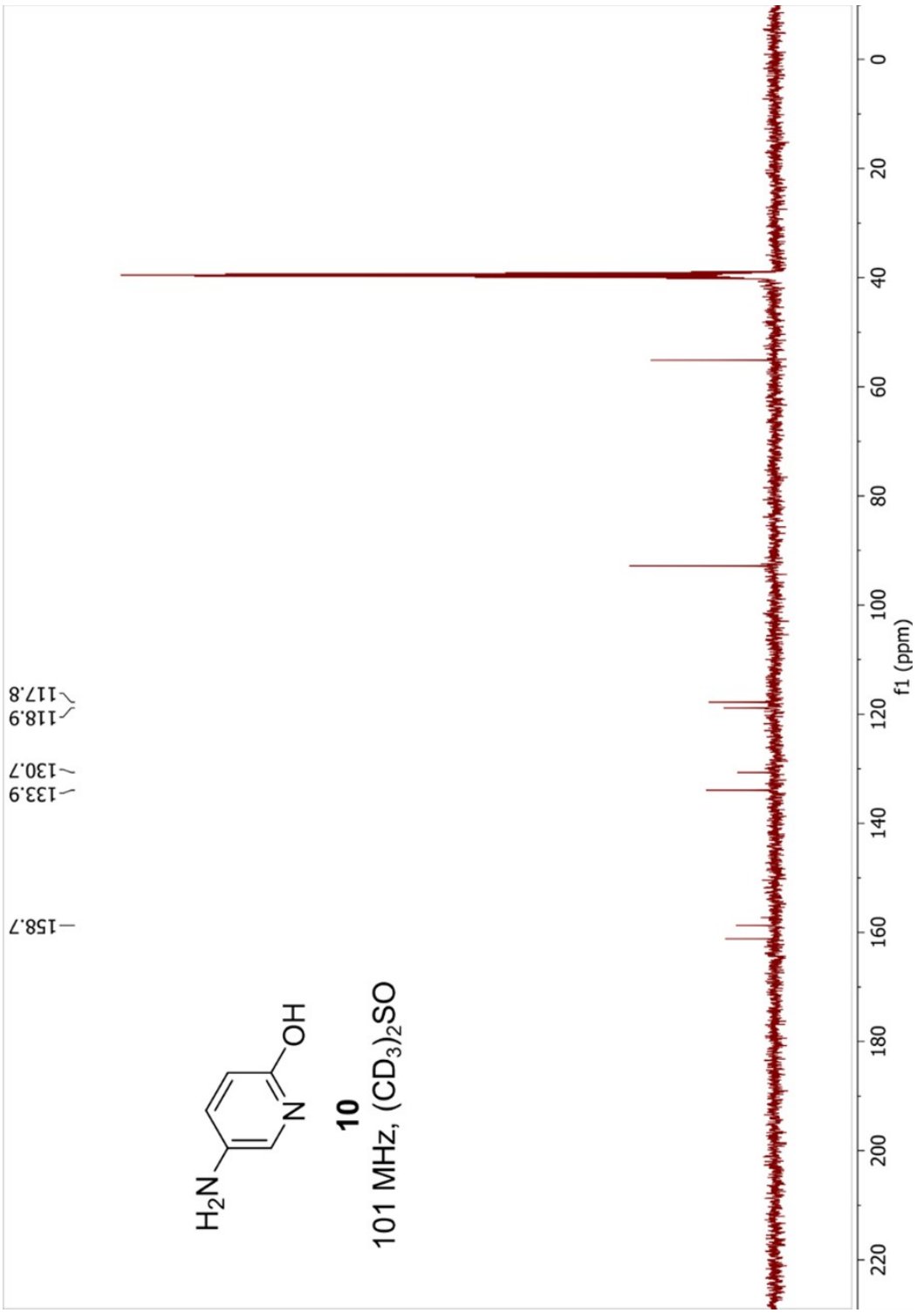

References

S1. Bausch, M.; Schultheiss, C.; Sieck, J. B. Recommendations for Comparison of Productivity Between Fed-Batch and Perfusion Processes. *Biotechnol. J.* 2019, *14* (2), 1700721.

S2. Yu, C.; Fu, J.; Muzzio, M.; Shen, T.; Su, D.; Zhu, J.; Sun, S. CuNi Nanoparticles Assembled on Graphene for Catalytic Methanolysis of Ammonia Borane and Hydrogenation of Nitro/Nitrile Compounds. *Chem. Mater.* 2017, *29* (3), 1413-1418.

S3. Yu, C.; Fu, J.; Muzzio, M.; Shen, T.; Su, D.; Zhu, J.; Sun, S. CuNi Nanoparticles Assembled on Graphene for Catalytic Methanolysis of Ammonia Borane and Hydrogenation of Nitro/Nitrile Compounds. *Chem. Mater.* 2017, *29* (3), 1413-1418.

S4. Göksu, H.; Ho, S. F.; Metin, Ö.; Korkmaz, K.; Mendoza Garcia, A.; Gültekin, M. S.; Sun, S. Tandem Dehydrogenation of Ammonia Borane and Hydrogenation of Nitro/Nitrile Compounds Catalyzed by Graphene-Supported NiPd Alloy Nanoparticles. *ACS Catal.* 2014, *4* (6), 1777-1782.

S5. Lu, B.-B.; Chen, X.-Y.; Feng, C.-J.; Chang, J.; Ye, F. Palladium Nanoparticles Immobilized on a Resorcin[4]arene-Based Metal-Organic Framework for Hydrogenation of Nitroarenes. *ACS Appl. Nano Mater.* 2021, *4* (2), 2278-2284.

S6. Sun, Q.; Wang, N.; Zhang, T.; Bai, R.; Mayoral, A.; Zhang, P.; Zhang, Q.; Terasaki, O.; Yu, J. Zeolite-Encaged Single-Atom Rhodium Catalysts: Highly-Efficient Hydrogen Generation and Shape-Selective Tandem Hydrogenation of Nitroarenes. *Angew. Chem., Int. Ed.* 2019, *58* (51), 18570-18576.

S7. Muzzio, M.; Lin, H.; Wei, K.; Guo, X.; Yu, C.; Yom, T.; Xi, Z.; Yin, Z.; Sun, S. Efficient Hydrogen Generation from Ammonia Borane and Tandem Hydrogenation or Hydrodehalogenation over AuPd Nanoparticles. *ACS Sustain. Chem. Eng.* 2020, *8* (7), 2814-2821.

S8. Shen, M.; Liu, H.; Yu, C.; Yin, Z.; Muzzio, M.; Li, J.; Xi, Z.; Yu, Y.; Sun, S. Room-Temperature Chemoselective Reduction of 3-Nitrostyrene to 3-Vinylaniline by Ammonia Borane over Cu Nanoparticles. *J. Am. Chem. Soc.* 2018, *140* (48), 16460-16463.

S9. Han, A.; Zhang, J.; Sun, W.; Chen, W.; Zhang, S.; Han, Y.; Feng, Q.; Zheng, L.; Gu, L.; Chen, C.; Peng, Q.; Wang, D.; Li, Y., Isolating contiguous Pt atoms and forming Pt-Zn intermetallic nanoparticles to regulate selectivity in 4-nitrophenylacetylene hydrogenation. *Nat. Commun.* 2019, *10* (1), 3787.

S10. Wang, Z.; Zhang, H.; Chen, L.; Miao, S.; Wu, S.; Hao, X.; Zhang, W.; Jia, M. Interfacial Synergy of PtPd Nanoparticles Dispersed on Amine-Modified ZrSBA-15 in Catalytic Dehydrogenation of Ammonia Borane and Reduction of p-Nitrophenol. *J. Phys. Chem. C* 2018, *122* (24), 12975-12983.

S11. Nişancı, B.; Turgut, M.; Sevim, M.; Metin, Ö. Three-Component Cascade Reaction in a Tube: In Situ Synthesis of Pd Nanoparticles Supported on mpg-C3N4, Dehydrogenation of Ammonia Borane and Hydrogenation of Nitroarenes. *ChemistrySelect* 2017, *2* (22), 6344-6349.

S12. Metin, Ö.; Mendoza-Garcia, A.; Dalmızrak, D.; Gültekin, M. S.; Sun, S. FePd alloy nanoparticles assembled on reduced graphene oxide as a catalyst for selective transfer hydrogenation of nitroarenes to anilines using ammonia borane as a hydrogen source. *Catal. Sci. Technol.* 2016, *6* (15), 6137-6143.
S13. Yang, Q.; Chen, Y.-Z.; Wang, Z. U.; Xu, Q.; Jiang, H.-L. One-pot tandem catalysis over Pd@MIL-101: boosting the efficiency of nitro compound hydrogenation by coupling with ammonia borane dehydrogenation. *Chem. Commun.* 2015, *51* (52), 10419-10422.
S14. Du, J.; Chen, J.; Xia, H.; Zhao, Y.; Wang, F.; Liu, H.; Zhou, W.; Wang, B. Commercially Available CuO Catalyzed Hydrogenation of Nitroarenes Using Ammonia Borane as a Hydrogen Source. *ChemCatChem* 2020, *12* (9), 2426-2430.
S15. Cheng, S.; Liu, Y.; Zhao, Y.; Zhao, X.; Lang, Z.; Tan, H.; Qiu, T.; Wang, Y. Superfine CoNi alloy embedded in Al_2O_3 nanosheets for efficient tandem catalytic reduction of nitroaromatic compounds by ammonia borane. *Dalton Trans.* 2019, *48* (47), 17499-17506.
S16. Chiba, S.; Zhang, L.; Lee, J.-Y. Copper-Catalyzed Synthesis of Azaspirocyclohexadienones from α-Azido-N-arylamides under an Oxygen Atmosphere. *J. Am. Chem. Soc.* 2010, *132* (21), 7266-7267.
S17. Yang, H.; Li, Y.; Jiang, M.; Wang, J.; Fu, H. General Copper-Catalyzed Transformations of Functional Groups from Arylboronic Acids in Water. *Chem. Eur. J.* 2011, *17* (20), 5652-5660.
S18. Li, J.; Shi, X.-Y.; Bi, Y.-Y.; Wei, J.-F.; Chen, Z.-G. Pd Nanoparticles in Ionic Liquid Brush: A Highly Active and Reusable Heterogeneous Catalytic Assembly for Solvent-Free or On-Water Hydrogenation of Nitroarene under Mild Conditions. *ACS Catal.* 2011, *1* (6), 657-664.
S19. Cantillo, D.; Baghbanzadeh, M.; Kappe, C. O. In Situ Generated Iron Oxide Nanocrystals as Efficient and Selective Catalysts for the Reduction of Nitroarenes using a Continuous Flow Method. *Angew. Chem., Int. Ed.* 2012, *51* (40), 10190-10193.
S20. Udumula, V.; Tyler, J. H.; Davis, D. A.; Wang, H.; Linford, M. R.; Minson, P. S.; Michaelis, D. J. Dual Optimization Approach to Bimetallic Nanoparticle Catalysis: Impact of M1/M2 Ratio and Supporting Polymer Structure on Reactivity. *ACS Catal.* 2015, *5* (6), 3457-3462.
S21. Wu, G. G.; Chen, F. X.; LaFrance, D.; Liu, Z.; Greene, S. G.; Wong, Y.-S.; Xie, J. A Novel Iodide-Catalyzed Reduction of Nitroarenes and Aryl Ketones with H_3PO_2 or H_3PO_3: Its Application to the Synthesis of a Potential Anticancer Agent. *Org. Lett.* 2011, *13* (19), 5220-5223.